Review



# Polycaprolactone Composites/Blends and Their Applications Especially in Water Treatment

Gizem Özge Kayan and Asgar Kayan *

Posted Date: 12 September 2023

doi: 10.20944/preprints202309.0709.v1

Keywords: polycaprolactone; blend; composite; adsorbent; degradation; wastewater

*Review*

# Polycaprolactone Composites/Blends and Their Applications Especially in Water Treatment

**Gizem Özge Kayan [1] and Asgar Kayan [2,*]**

[1] Metallurgical & Materials Engineering Department, Faculty of Chemical and Metallurgical Engineering, Istanbul Technical University, Maslak, Istanbul 34469, Turkey; E-mail (Gizem Özge Kayan): kayangi@itu.edu.tr

[2] Kocaeli University, Department of Chemistry, Izmit, Kocaeli 41380, Turkey

* Correspondence: akayan@kocaeli.edu.tr; Tel.: +90 2623032032; Fax: +90 2623032003

**Abstract:** Biodegradable poly(ε-caprolactone) (PCL) and its composites or blends have gotten a lot of attention in the last decade because of their potential applications in human life and environmental remediation. As a result, there is a growing interest in the synthesis of PCL-composites/blends and their applications. Greater efforts have been made to develop biodegradable chemical materials as adsorbents that do not pollute the environment in order to replace traditional materials. Among the numerous types of degradable materials, PCL is currently the most promising, the most popular, and the best material to be developed, and it is referred to as the "green" eco-friendly material. Membranes and adsorbents for water treatment, packaging and compost bags, controlled drug carriers, biomaterials for tissues such as bone, cartilage, ligament, skeletal muscle, skin, cardiovascular and nerve tissues are just some of the applications of this biodegradable polymer (PCL). The goal of this review is to present a brief overview of PCL, its properties, syntheses of PCL, PCL composites, and PCL blends, but to provide a detailed investigation into the utility of PCL/PCL-based adsorbing agents in the removal of dyes/heavy metal ions.

**Keywords:** polycaprolactone; blend; composite; adsorbent; degradation; wastewater

## 1. Introduction

In recent years, various polymers have been employed to create composites, blends, and membranes for water treatment and remediation [1]. However, these polymers are not biodegradable and must be disposed of in the environment, which is another issue for waste management [2]. Biodegradable polymers, which decompose easily, may be the best alternative for these materials. Biodegradable polymers include both natural polymers and synthetic polymers as classified in Figure 1 [3–5]. PCL is a widely recognized biodegradable and biocompatible petroleum-based polymer with numerous applications in packaging, scaffolds, prosthetics, sutures, drug delivery, films, carry bags, pouches, trays, reusable dishes, membranes, and other fields. PCL can be degraded without polluting the environment by hydrolysis of ester bonds or by microorganisms [6]. PCL is easily blended with other polymers and is soluble not in water but in a number of different organic solvents [7]. In addition to the applications mentioned above, PCL can be used in water treatment plants as it is a biocompatible, biodegradable and environmentally friendly polymer.

Preprints (www.preprints.org) | NOT PEER-REVIEWED | Posted: 12 September 2023 doi:10.20944/preprints202309.0709.v1



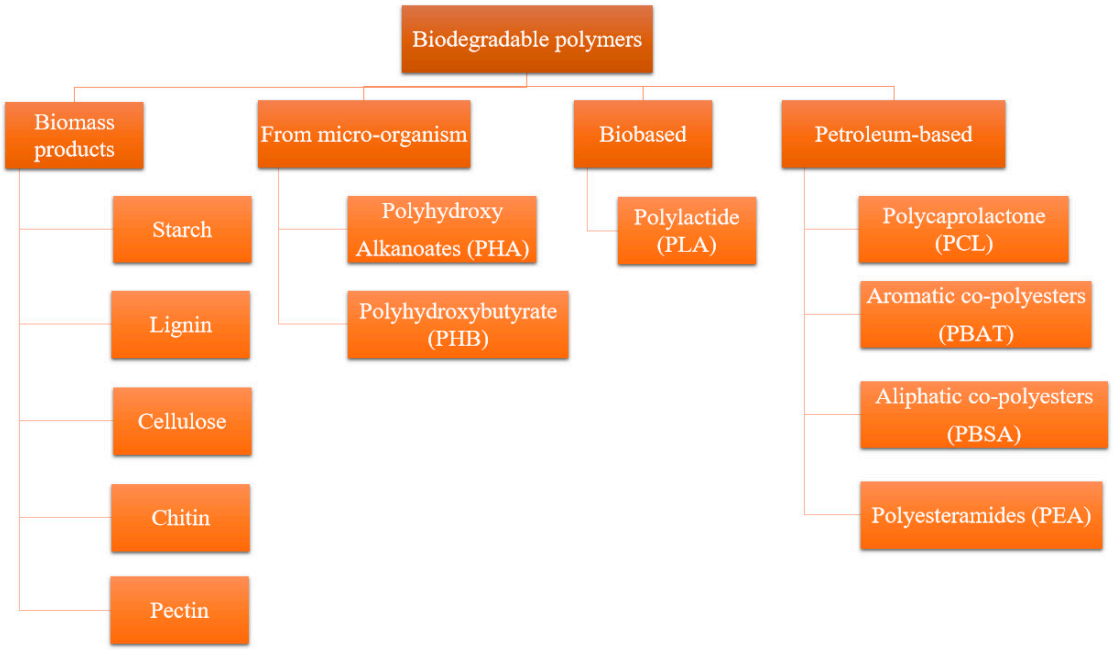


**Figure 1.** Classification of natural and synthetic biodegradable polymers [3–5].

However, reinforcing fillers are required to improve the performance of the PCL matrix by increasing its mechanical, chemical, and thermal properties, as well as to broaden its application to other fields [8]. As a result, PCL was investigated by interacting with various loading agents. In particular, studies of mixtures of cellulose, chitosan, alginate, metal oxides, zeolites, and biodegradable polymers to obtain blends or composites to resolve some of the noted drawbacks of PCL have been reported [9]. Besides the fillers added to PCL, PCL itself can be used as filler. Some properties are also expected of PCL reinforcing fillers. For instance, low-cost, biodegradable, renewable resources, high strength, low density, and easy-to-process materials are desired. It is also desirable to have a homogeneous mixture or powerful interplay between the polymer matrices and the reinforcing agents. Because of their dissimilar properties, these materials can be difficult to interact with each other. To give an example of this dissimilarity, cellulose fibers are difficult to dissolve and disperse in the PCL matrix because of the hydrophilicity of cellulose fibers and the hydrophobicity of PCL [10]. In order to improve the cellulose fiber dispersion in PCL, chemical treatments are applied to the fiber surface to increase its chemical and physical interaction with the PCL matrix. This problem is solved by applying chemical treatments to the fiber surface to improve the cellulose fiber dispersion in PCL. This improvement in compatibility provides better interface interaction that improves composite mechanical performance [11]. In short, when PCL is combined with other polymers, it changes their biodegradability and mechanical properties [12]. The majority of literature reviews have focused on PCL applications varying from sutures [13] to wound dressings [14], artificial blood vessels [15], nerve regeneration [16], bone engineering [17], food packaging systems [18], membrane [19] and drug delivery devices [20]. There is, however, no systematic and up-to-date review of PCL applications for heavy metal ions and dyes removal from wastewater.

Several studies have taken place over the last decade to explore the possibility of improving the PCL properties through the use of other biopolymers and metal oxides for their use in removing pollutants from aqueous solution. Keeping the preceding discussion in mind, the current review paper was written with the goal of summarizing recent applications of PCL in adsorbent and membrane production in a comprehensive manner. Meanwhile, the synthesis, degradation, mechanical properties, and some other applications of PCL will be briefly mentioned.

Preprints (www.preprints.org) | NOT PEER-REVIEWED | Posted: 12 September 2023 doi:10.20944/preprints202309.0709.v1



## 2. Chemical Synthesis of PCL

PCL is a non-hazardous and non-biobased aliphatic polyester [21]. Commercially, PCL is produced from crude oil via two ways: (i) polycondensation of 6-hydroxyhexanoic acid ($C_6H_{12}O_3$) [22] and (ii) ROP of ε-CL ($C_6H_{10}O_2$) monomer with tin octoate, transition metal alkoxides or their derivative catalysts [23]. If the catalyst does not act as the initiator, low molecular alcohols are employed to help regulate the molecular weights that define the polymer's properties [24]. For instance, PCL with a molecular weight ($M_w$) of around 80.000 Da has plastic properties, whereas PCL with $M_w$ of 10.000 Da is inherently very hard and brittle [25].

PCL is synthesized in the first method through polycondensation reactions of 6-hydroxyhexanoic acid in the presence of suitable catalysts and continuous removal of water under vacuum. The synthesis reaction is typically completed in a few hours at temperatures ranging from 80 to 150 °C. This synthesis method typically yields a low molecular weight with a broad polydispersity index and low quality polymer (Scheme 1) [22].

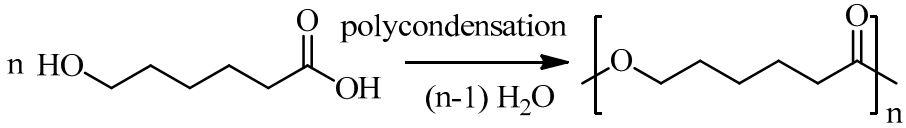


**Scheme 1.** Synthesis of PCL with polycondensation reactions.

ROP, on the other hand, is preferred in industry for PCL production because it provides controllable polymerization, a higher molecular mass, and a lower polydispersity index polymer. Anionic, cationic, and coordination-insertion catalysts are the three types of catalysts used in the ROP of ε-caprolactone. Because these three types of catalysts work in different ways, they result in the formation of polymers with varying structures and sizes.

As catalysts for ε-caprolactone anionic ring-opening polymerization, various alkali metal salts (*t*-BuOK, *i*-PrOK, KH, PhLi, and *i*-$Pr_2$NLi, among others) were used [26]. The ring opens solely in the acyl-oxygen position in anionic polymerization of ε-CL, and the species produced by the growth are alkoxide anions. The major disadvantage of this process is the presence of significant intramolecular transesterification in the final stage of the polymerization, also known as ''backbiting''. If polymerization is not stopped before backbiting, the resulting polymer has a smaller molecular weight ($M_w$) or a cyclic structure. Anionic polymerization, on the other hand, allows for the controlled synthesis of high $M_w$ polymers in a polar solvent.

Cationic ROP includes the creation of a positively charged species that is attacked by the monomer's carbonyl oxygen. The attack causes the positively charged species to ring-open via $SN_2$-type mechanisms [27,28]. Cationic polymerization is a difficult method to control and frequently results in low molecular weight polymers or oligomers. Cationic polymerization can be carried out using catalysts such as cationic heteroscorpionate aluminum complexes, mono- and bis(phosphinophenolate) aluminum cationic complexes [29], Trityl tetrafluoroborate ($Ph_3CBF_4$) [30], and iron (III) chloride ($FeCl_3$) or $FeCl_3/nH_2O$ systems [31].

The last mechanism is coordination-insertion ROP, which is a quasi-anionic ROP [32]. As illustrated in Scheme 2, the ε-caprolactone monomer first binds to the metal center through the carbonyl (C=O) oxygen atom. The catalyst's nucleophilic alkoxide group is then coordinated to the activated carbonyl group of ε-caprolactone, resulting in cleavage of the acyl-oxygen bond. Following ε-caprolactone monomers bind to the metal center and insert into the metal-alkoxide bond, resulting in PCL formation. The most commonly used catalysts in ROP are tin octoate [33], metal alkoxides such as aluminum [34], tin [35], zirconium [36], titanium [37] alkoxides, rare earth metal alkoxides and derivatives containing coordinated Lewis base $Ln(OR)_3(L)_n$ (L = 2,2′-bipyridyl, n = 2, 1,10-phenanthroline, n = 1, 18-crown-6 ether, n = 1) [38], transition metal(TM)-carboxylates as in zinc(3,5-dimethylpyrazole)carboxylates [39], TM-phenolates like titanium compounds [$LTiX_2$] bearing a sulfide-linked bis(phenol) ligand [L= OSSO type ligand] [40,41], TM-Schiff base complexes such as LLa($OC_6H_2$-2,6-$^t$Bu$_2$-4-$CH_3$)(THF), LLaO$^t$Bu(THF), [LLaO$^i$Pr]$_2$, [LLaOBn]$_2$, and [LLaOEt]$_2$ (L= NH($CH_2CH_2$N =

Preprints (www.preprints.org) | NOT PEER-REVIEWED | Posted: 12 September 2023 doi:10.20944/preprints202309.0709.v1



$CHC_6H_2$-3,5-$^t$Bu$_2$-2-O)$_2$) [42]. ε-CL was recently initiated by exfoliated oxidized biochar (Eoxbc). The surface hydroxyl groups (OH) on Eoxbc are enough to start and promote the ROP of ε-CL using stannous octoate, bases or enzymes as catalysts [43].

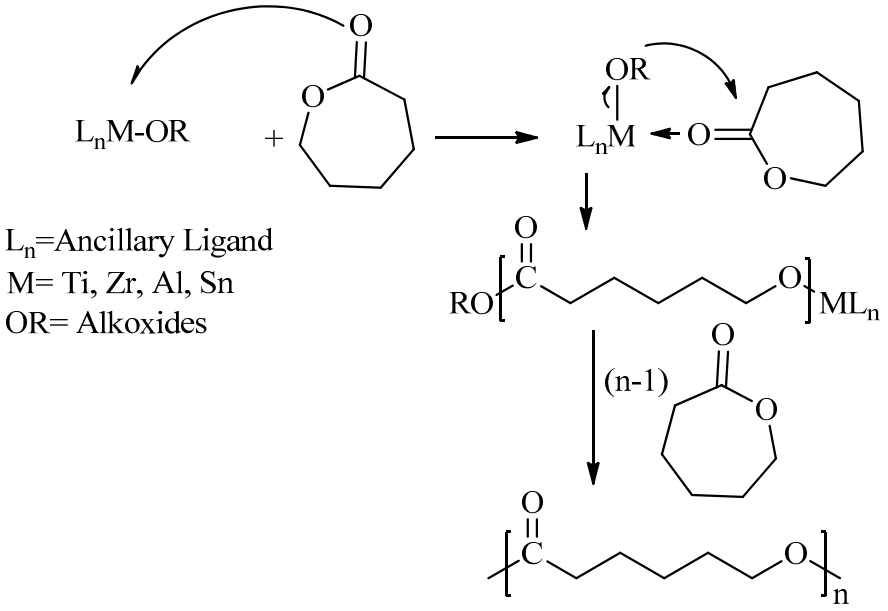


**Scheme 2.** Synthesis of PCL by ring-opening polymerization [23,37].

Some spectroscopic properties of PCL can be summarized as in Table 1.

**Table 1.** Spectroscopic data related with PCL [37].

| | |
|---|---|
| $^1$H-NMR results (in $CDCl_3$) | δ(ppm): 4.1 (t, *J* = 6.7 Hz, $^{\varepsilon}CH_2O$), 2.3 (t, *J* = 7.5 Hz, $^{\alpha}CH_2$), 1.6 (m, *J* = 7.3 Hz, $^{\beta,\delta}CH_2$), 1.4 (m, *J* = 7.3 Hz, $^{\gamma}CH_2$) |
| $^{13}$C NMR results (in $CDCl_3$) | δ(ppm): 174 (C=O), 64 ($^{\varepsilon}CH_2O$), 34 ($^{\alpha}CH_2$), 28 ($^{\delta}CH_2$), 26 ($^{\beta}CH_2$), 25 ($^{\gamma}CH_2$). [O=C-$^{\alpha}CH_2{}^{\beta}CH_2{}^{\gamma}CH_2{}^{\delta}CH_2{}^{\varepsilon}CH_2O$-]. |
| FTIR results (cm$^{-1}$) | 2936 (CH, asym str), 2865 (CH, sym str), 1723 (C=O, asym str), 1472, 1418, 1394, 1366 (C=O, sym str) 1288, 1240 (C–O–C str vib), 1162 (C–O–C str vib), 1100, 1046, 1018 cm$^{-1}$ etc. |

Of all the synthesis methods, the coordination-insertion ROP method is the most common and suitable process for the polymerization of ε-caprolactone. PCLs obtained by this method have high molecular weights and narrow polydispersity indices.

### 3. Degradation of PCL

PCL biodegrades depending on the amount crystallinity, polymer molecular mass, and other degradation parameters such as environment, temperature, pH, and salinity [25]. Because there are more hydroxyl groups present at higher pH, the rate of degradation will therefore be higher. However, the existence of hydrophobic $CH_2$ units as the recurring moiety in PCL significantly hinders its degradation kinetics, leading to a notably protracted degradation timeline, typically spanning over 2-3 years.

Preprints (www.preprints.org) | NOT PEER-REVIEWED | Posted: 12 September 2023 doi:10.20944/preprints202309.0709.v1



PCL undergoes degradation through two common pathways: (i) enzymatic degradation (also called surface erosion mechanism) and (ii) hydrolytic degradation (also known as bulk erosion mechanism) (Figure 2) [25,44].

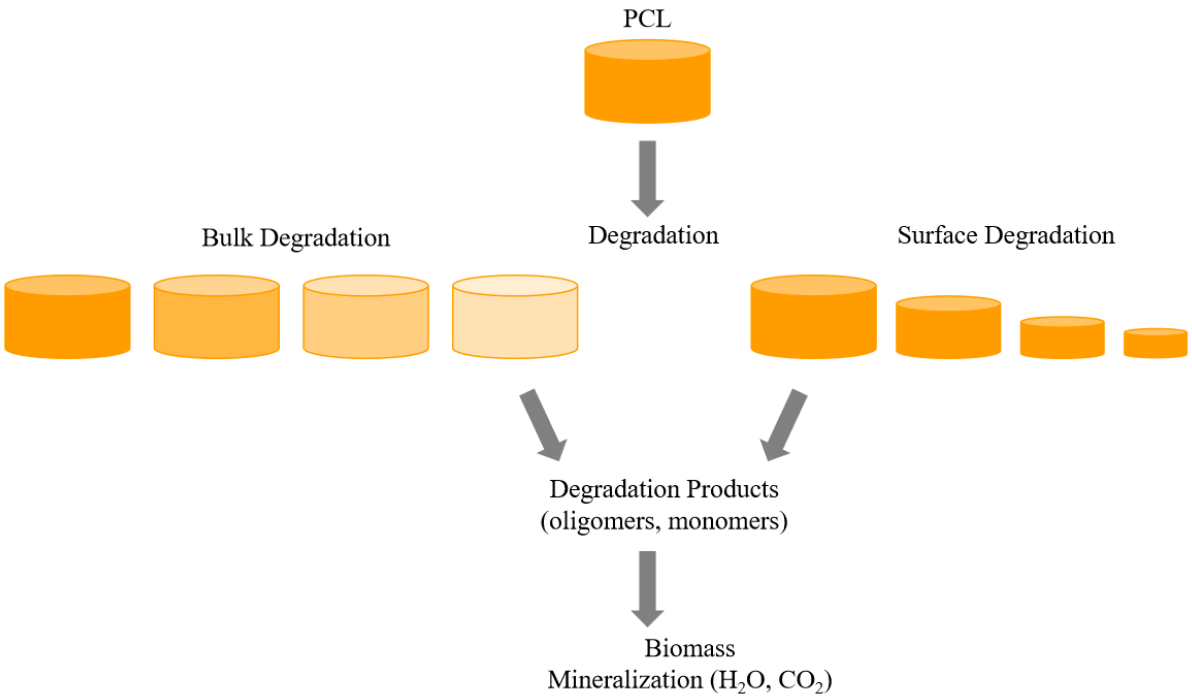


**Figure 2.** Bulk and surface degradation of PCL [25,44].

Surface enzymatic erosion degrades PCL with significant mass loss but very little change in molecular weight. Surface erosion of PCL refers to the hydrolytic degradation of the polymer backbone solely at the PCL surface, wherein the speed of hydrolytic chain scission and the synthesis of monomers and oligomers are faster than the speed of water penetration within the polymer bulk, leading to polymer thinning without observable impact on its molecular weight. In other words, surface erosion is expected if bond hydrolysis happens faster than water diffusion.

The enzymatic degradation is primarily carried out by the enzyme lipase (which can be found in both fungi and bacteria) at chain ends, folds, and edges of crystals, in which chain mobility is greater [25]. The enzyme works by cleaving PCL ester bonds. Khan et al. investigated the PCL degradation adequacy of three different Lactobacillus lipases and discovered that PCL degradation depends on enzyme concentration and type [45]. Aris et al. investigated the hydrolysis of PCL ($M_n$: 10.000 Da) by Candida antarctica lipase B (CALB) in organic solvent and discovered that rising PCL concentration decreased degradation rate while increasing reaction temperature from 30 to 50 °C increased it [46]. Ma et al. used Candida antarctica lipase to degrade PCL films with three distinct molecular weights, and the findings indicated that lipase activity was unaffected by the molecular weights of the PCL films. But as the molecular weight increased, more pores appeared in the degraded PCL films, and as the degradation time lengthened, the pores grew deeper [47].

Hydrolytic degradation (bulk erosion) reduces the molecular weight of PCL while causing minor mass loss. This degradation mode involves the penetration of water throughout the entirety of the polymer bulk, instigating hydrolysis and consequent random hydrolytic chain scission that eventually leads to a reduction in molecular weight [48]. Since the cleavage occurs in the non-crystalline region, the crystallinity of the polymer increases. The bulk of the polymer is diffused out by the monomers or oligomers, causing slower polymer erosion and more pronounced bulk degradation. As a result, internal polymer degradation is faster than surface polymer degradation. In other words, bulk erosion occurs when the speed of water diffusion surpasses the speed of bond hydrolysis. Bulk erosion has been reported in aliphatic polyesters such as PCL. Although mass loss is low in this type of erosion, cracks form in the sample, threatening mechanical functionality [48].

Preprints (www.preprints.org) | NOT PEER-REVIEWED | Posted: 12 September 2023 doi:10.20944/preprints202309.0709.v1



Under controlled conditions, the biodegradability of pure PCL, its blends and nanocomposites was investigated in different enzyme, pure microorganism (fungi), organic manure, Ganges water, and basic buffer solution. The rate of PCL biodegradation in nanohybrids has increased significantly and is highly dependent on the working environment and the chemicals used [49]. The pH of the system affects the rate of degradation. PCL degrades faster in an alkaline environment than in an acidic environment [48]. These enzymatic and hydrolytic degradations produce polymers with a lower molecular weight (3000) and 6-hydroxycaproic acid, resulting in smaller particles. As a result, polymer biodegradation produces fragmentation compounds and is considered complete when $H_2O$ and $CO_2$ are produced by microbial action as seen in Figure 3 [49,50].

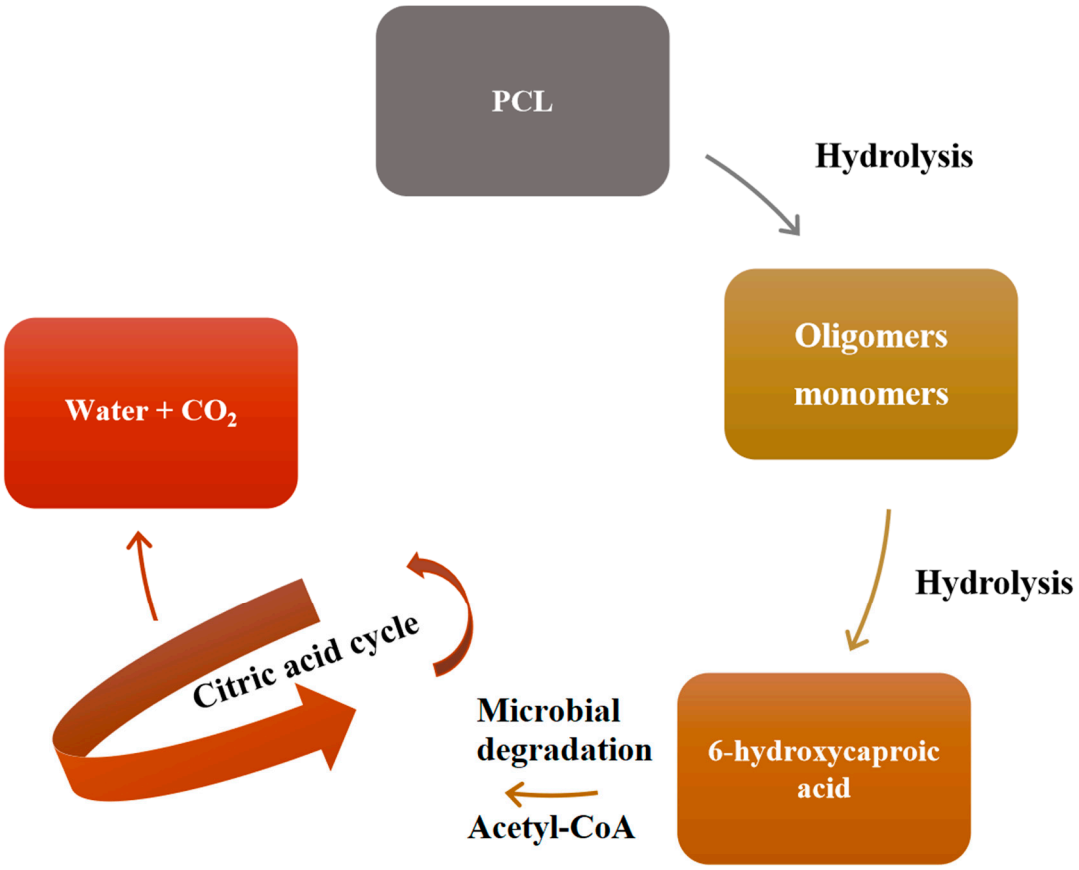


**Figure 3.** Biodegradation mechanism of PCL [49,50].

Because of its hydrolytic nature, PCL's slow degradation rate can be accelerated up by adding other polymers or degradation catalysts. Polymers such as lactide, glycolide, succinic acid, and other natural fibrous materials can be employed to improve the degradation rate [51,52].

## 4. Material Properties of PCL

Polycaprolactone (PCL) is a semicrystalline aliphatic polyester which has glass transition temperature ($T_g$) of -60°C, a melting point between 58 and 64 °C depending on its crystalline structure, and degradation time approximately 2-3 years [53]. PCL is extremely tough because of the presence of amorphous regions in rubbery state. The low melting temperature of PCL and its depolymerization at high temperatures (>200°C) are the main disadvantages for its utilization, which can be overcome by cross-linking or blending with the other polymers [54]. PCL can be graded according to molecular weights and shows different physical and mechanical characteristics depending upon molecular weights. For examples, PCL with a molecular weight of about 40.000 Da is hard and extensible, while PCL with a molecular weight of between 10.000 Da (PCL-300) and 5000 Da (PCL-150) is pretty hard and brittle. In the industrial setting, PCL-700 is preferred for blending because the end

Preprints (www.preprints.org) | NOT PEER-REVIEWED | Posted: 12 September 2023 doi:10.20944/preprints202309.0709.v1



functional groups play a significant role in affecting blendability and compatibility when the molecular weight is reduced [25,55]. The crystallinity of PCL tends to decline with increasing molecular weight. PCL's great solubility in some organic solvents, low melting point and exceptional blend-compatibility has sparked in-depth investigation into its potential use in the biomedical area [56].

PCL's mechanical, physical, thermal, biodegradable, and biocompatible properties are entirely determined by its crystallinity and molecular weight. Because of its superior rheological and viscoelastic properties, the Food and Drug Administration (FDA) has approved its use in a variety of long-term degradable medical appliance and implants. The medical device industry was searching for biodegradable PCL to replace metal implants (such as nails, screws, plates, etc.) [57]. PCL crystallization and morphologic properties are extremely important. PCL is a semicrystalline aliphatic polyester and relatively hydrophobic polymer with a variety of properties [53,58,59], as shown in Table 2. As the molecular mass increases, the crystallinity level is expected to decrease. PCL's lower glass transition ($T_g$) and melting ($T_m$) temperatures make it easy to form at low temperatures. In some organic solvents such as benzene ($C_6H_6$), carbon tetrachloride ($CCl_4$), chloroform ($CHCl_3$), cyclohexanone ($C_6H_{10}O$), methylene chloride ($CH_2Cl_2$), isonitropropane ($C_3H_7NO_2$), and toluene ($C_7H_8$), PCL is quickly soluble at RT. However, it dissolves poorly in solvents like acetone($C_3H_6O$), acetonitrile ($C_2H_3N$), 2-butanone ($C_4H_8O$), dimethyl formamide ($C_3H_7NO$), and ethyl acetate ($C_4H_8O_2$) [44,60,61]. Heating to 50°C can improve its solubility in these solvents. PCL is insoluble in water ($H_2O$), ethyl alcohol ($C_2H_6O$), diethyl ether ($C_4H_{10}O$) and petroleum ether ($C_6H_{14}$) [60].

**Table 2.** A list of PCL's mechanical and physical characteristics [53,58,59].

| Properties | Values |
|---|---|
| Molecular weight, $M_n$, g/mol | $3x10^3$ to $8x10^4$ |
| Density, g/cm$^3$ | 1.07 to 1.20 |
| Melting temperature ($T_m$), $^oC$ | 56 to 65 |
| Glass transition temp. ($T_g$), $^oC$ | -65 to -60 |
| Decomposition temp. ($T_d$), $^oC$ | 350 |
| Degradation time, years | 2-3 |
| Inherent viscosity, cm$^3$/g | 100–130 |
| Intrinsic viscosity, cm$^3$/g | 0.9 |
| Tensile strength, $\sigma_m$, MPa | 4-785 |
| Tensile elastic modulus, $E_t$, MPa | 250-440 |
| Yield stress, $\sigma_y$, kN/m$^2$ | $8.2x10^3$-$1.1x10^4$ |
| Young modulus, MPa | 210-440 |
| Elongation at break, % | 20–1000 |
| Conformation | Extended and zigzag |
| Degree of crystallinity | Semicrystalline (50%) |
| Water vapor permeability, g/m$^2$·day | 783 |
| Oxygen transmission rate, m$^3$/m$^2$·day | 486 |

When the mechanical values in Table 2 are examined, it can be seen that PCL exhibits noticeably low tensile strength and modulus, but a high elongation at break. Because of its physical and mechanical characteristics, miscibility with many different polymers, biodegradability, and ability to form composites, PCL is an important bioplastic polymer. It can be combined with other plastic polymers and oxide materials to improve adhesion, dyeability, and stress crack resistance. As seen in Figure 4, bioplastics are divided into three categories. Of these classifications, biopolymers that are both petroleum-based and biodegradable are poly(ε-caprolactone) (PCL), poly(butylene-adipate-co-terephthalate) (PBAT), and poly(vinyl alcohol) (PVA). Bio-based and biodegradable ones are poly(lactic acid) (PLA), poly(hydroxy alkanoate) (PHA), poly(butylene succinate) (PBS), and starch blends. Bio-based and non-biodegradable ones are polyethylene (PE), polyamide (PA),

Preprints (www.preprints.org) | NOT PEER-REVIEWED | Posted: 12 September 2023 doi:10.20944/preprints202309.0709.v1



poly(trimethylene terephthalate) (PTT) and polypropylene (PP), poly(ethylene terephthalate) (PET) [62,63]. Some polymers, such as polyethylene, can be both bio-based and petroleum-based.

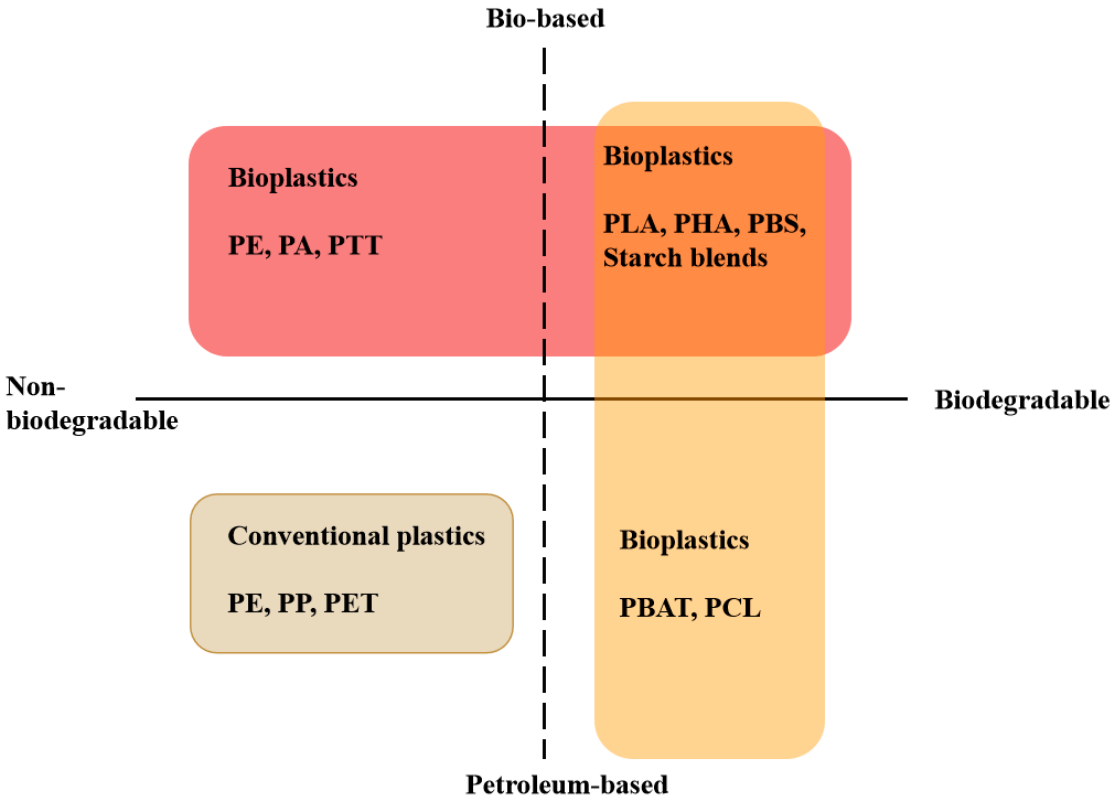


**Figure 4.** Biodegradable and non-biodegradable plastics [61–63].

## 5. PCL Blends/Composites

### *5.1. PCL Reinforced with Other Polymers*

Polymer blends have been employed as a substituent because of the low mechanical properties, low thermal stability, low adsorption capacity, and hydrophobic properties of homo-PCL [64,65]. Numerous studies have shown that combining PCL nanofibers with other polymers such as cellulose, nitrocellulose, cellulose butyrate, chitosan, chitin, alginate, and pectin improves its physical properties. Cellulose is a low-cost, widely available material that is both renewable and biodegradable. The researchers looked into how cellulosic filler type and ingredients affected the mechanical characteristics of PCL-based composites [66]. The mechanical characteristics of PCL composites were found to be modulated by multiple interdependent factors, including chemical suitability, interfacial strength, filler dispersion, and padding aspect ratio [67]. Because of the hydrophilic surface of the cellulose-based nano reinforcement particles, the interaction between the template and the padding is poor. Chemical suitability is critical in managing dispersion and adhesion between them. As a result, weak padding-template interactions are common when hydrophilic paddings like cellulose nanocrystal (CNC), cellulose nanofiber (CNF), and bacterial nanocellulose (BC) are added to hydrophobic templates (PCL, PLA, etc.). These issues, however, can be mitigated by a variety of surface adjustments [53].

In terms of thermal stability and mechanical properties, PCL nanocomposites strengthened with cellulose nanocrystals (CNCs) (surface modified by covalent grafting or physisorption) outperformed better than unfilled PCL and nanocomposites with unmodified CNCs. PCL strengthened with grafted CNCs had a higher degradation temperature than micelle-modified CNCs, which had a higher degradation temperature than latex-adsorbed CNCs with a long PBMA chain length. In terms of thermal and mechanical characteristics of the final nanocomposite, the finding obviously show

 doi:10.20944/preprints202309.0709.v1



that covalent grafting outperforms physisorption. This one-of-a-kind study will be extremely useful in the future design of PCL/CNC-based composites with customized features [68]. The morphological analyses performed revealed a reasonable distribution of cellulose nanofibers (CNFs) within the PCL template, as well as high reliability among the fabricated scaffolds. Remarkable impacts on surface wettability and thermal features have been observed for scaffolds. In terms of mechanical features, reinforced scaffolds had higher scaffold stiffness [69].

The cellulose acetate nanofiber (CANF) and the cellulose nanofiber (CNF) were produced as reinforcing materials for PCL. CANF was prepared by electrospinning and CNF was obtained by the deacetylation of the electrospun CANF. The CANF and CNF were then compressed separately into PCL as reinforcing compounds to yield CANF/PCL and CNF/PCL composites. The fracture-surface SEM micrographs showed that CANF is more compatible with the PCL matrix than CNF. The mechanical features of CANF/PCL and CNF/PCL were investigated, and it was discovered that both the fracture stress and the Young's modulus were extremely improved over pure PCL. Pure PCL had a Young's modulus (E) of about 250 MPa. More specifically, the fracture stress and Young's modulus of PCL increased by factors of 1.9 and 3.0 (E: 750 MPa), respectively, when 35 wt% of CANF was added to PCL. By adding the same amount of CNF, they became 2.6 and 4.5 ($E_{CNF/PCL}$: ~1100 MPa) times higher, respectively, by comparison to those of pure PCL due to the extremely high Young's modulus of CNF [61]. Successful ring-opening copolymerization was performed by adding 4-dimethylaminopyridine as a catalyst to tetrabutylammonium acetate/dimethyl sulfoxide solvent mixtures, and microcrystalline cellulose grafted PCL (MCC-G-PCL) was produced. By adding graphene oxide (GO), a new UV-shielding film based on MCC-g-PCL was created. This study offers a framework for creating UV-shielding polymers based on cellulose and for better comprehending the UV-shielding mechanism [70].

Twin-screw extrusion was used to create PCL/CNC nanocomposites at various CNC contents. Using a microcellular injection molding technique and $CO_2$ as the blowing agent, the nanocomposites were foamed. FTIR and Raman measurements revealed that the PCL matrix and CNCs interreacted, creating a robust interface between the two. In the foaming process, the CNCs productively served as nucleating agents, resulting in smaller pores and higher pore density with a higher CNC ingredient. PCL/CNC nanocomposites with 1% CNC showed higher yield stress (16.50 MPa for PCL and 17.40 MPa for 1 % CNC), tensile modulus (~184 MPa for PCL and ~200 MPa for 1% CNC), complex viscosities, and higher storage moduli because of the strengthening impact of CNCs. The adding of CNCs resulted in a decrease in the decomposition temperature ($T_d$, 411.4 ± 0.4 for PCL and 409.3 ± 0.7 for 1% CNC) but an increase in the glass transition temperature (Tg, 2 °C higher than that of pure PCL), crystallization temperature (Tc, from 34.2 ± 0.4 to 35.6 ± 0.9 °C), and crystallinity ($\chi_c$, from 39.0 ± 0.8 to 40.6 ± 1.0%) of PCL. The findings suggested that at 0.5% and 1% CNC contents, the nanocomposites were appropriate for cell growth, while at 5% CNC contents, cell death increased, primarily because of the sulfonic acid groups on the CNCs. The biocompatibility of the nanocomposites would be enhanced by further CNC modification. [71].

Hashiwaki et al. used hot-press molding to create thermoplastic blend films made of PCL and chitin butyrate (ChB) (50:50) [72]. The film properties changed depending on how much chitin was butyryl substituted. They tested various degrees of butyryl substitution with chitin, which had a 5% degree of deacetylation and found that high degrees of substitution led to improved miscibility with PCL. The PCL-ChB ratios can be changed to alter the mechanical stability of the films utilized as thermoplastic scaffolding substance. Especially, the partially miscible blend displayed the highest ductility attributable to a balance in the size and dispersion of the PCL microcrystals and the domain size of the blend components. This blend structure strengthens the physical and chemical features of the two materials by combining them [73].

PCL and chitosan (CS) are the two polymers most frequently encountered in biomedical applications. In this research, Sani et al. (2021) proposed graft work to solve the problem of finding co-solvents, which is the biggest challenge in PCL/CS blending studies. PCL/CS graft polymer instead of blend was synthesized and used in the production of bone tissue engineering scaffold. In addition, hydroxyapatite nanoparticles (nHAP, 1, 3, 5 and 10% w/w) were added to the PCL/CS graft polymer

to enhance the bioactivity and mechanical features of the scaffold. Elongation at break decreased significantly from 546 ± 24% for 1% nHAP to less than 100% for specimens including 3, 5, and 10% w/w nHAP. Tensile test in bulk and fiber state revealed that the porosity, fiber diameter and distribution had an important consequence on mechanical features of graft polymer. Besides, the mineralization and deterioration of the scaffold immersed in simulated body fluid (SBF) and phosphate-buffered saline (PBS) are accelerated by both CS-g-PCL and nHAP [74].

Sustainable PCL composites was produced by using exfoliated oxidized biochar (Eoxbc) as a bio-based filler. In the existence of both Eoxbc and $Sn(Oct)_2$, the conversion of ε-caprolactone to PCL increased from 55% to 88% and but the molecular weight of PCL decreased from 31.400 Da to 13.000 Da under the same reaction conditions. When compared to pure PCL, the novel materials created here have higher percentages of crystallinity and stiffness. At a comparatively high maximum temperature ($T_{max}$) of 288 °C, neat PCL only exhibits one primary degradation step. But compared to the neat polymer, PCL/Eoxbc composites had lower $T_{max}$ and were consequently less thermally stable. In this study, they reported the first try to enhance PCL mechanical characteristics and increase its degradability using a sustainable strategy driven by biochar incorporation [43].

The thermoplastic waxy starch (TPS) phase mixed with PCL, 70/30 (w/w), was combined with cellulose nanocrystals (CNCs) as reinforcing agents by higher shear rate co-rotating extrusion. In terms of TPS mass, nanocomposites were created using 3.25%, 6.5%, and 13 % by weight CNCs. In comparison to the TPS/PCL matrix, the nanocomposite with only 3.25 wt% CNCs increased the tensile strength by at least 3 times and the elastic modulus by more than 6 times, reaching values close to 12 MPa and 1.0 GPa, in order. Furthermore, the lower number of CNCs ensured the thermal stability of the TPS/PCL nanomaterials (250 °C), with a 20 °C increase in $T_{onset}$ compared to the neat matrix [75].

Peterson et al. carried out the synthesis of block polymer beads by PVA(aq) suspension polymerization to produce PCL-b-poly(styrene-co-divinylbenzene) beads, which can be electively etched under basic environments to obtain mesoporous polymer microspheres with constant pore size. The resulting microphase separation method produced a nanostructured diul-continuous morphology. The particle size (from 60 to 300 μm) by stirring speed and pore size (from 6 to 11 nm) by the molar mass of the PCL block polymer were independently tunable: BET measurement showed that the beads surface area were approximately 300 $m^2 g^{-1}$ when using a PCL macro-chain transfer agent (macroCTA) of 13 kg $mol^{-1}$. The beads formed were all on the micrometer length scale and did not have an impermeable skin layer. They have also succeeded in incorporating functional pore walls into the beads utilizing multiblock starting polymers. These functionalized beads showed high interest for organic dyes such as toluidine blue and methyl red in aqueous solution and captured dye from solution at rates faster than of mercantile ion exchange resins [76].

Electrospinning was used to create a PCL superamphiphobic perfluorooctyl acrylate (PCL-b-PTFOA) nanofiber film with a hierarchical porous surface. Because of its hierarchical pore morphology and low surface energy composition, the PCL-b-PTFOA nanofiber membrane could repulse a variety of solutions comprising water, coffee, and oil solutions. When compared to the PCL nanofiber membrane, the elongation at break of the PCL-b-PTFOA increased from 152.97% to 678.15%, the tensile strength increased from 4.11 to 5.78 MPa, and the membrane's super amphiphobicity was not ended up losing with a strain of up to 600% [77].

### *5.2. PCL Reinforced with Metal Oxides*

The membranes separation processes have played very important roles in water treatment plants. Membranes are made of biocompatible, non-toxic, and environmentally friendly materials such as PCL and some natural polymers. Nano or microfiber (2-6 μm) electrospun membranes combining PCL (15% w/v) with zeolite (20 w/v) were fabricated by using the multilayer electrospinning technique and used for water treatment processes. The resulting membrane (PCL/zeolite) had an average contact angle of 119.53±5.24 degrees. Angles greater than 90 degrees indicate that the membrane has a low wetting tendency, that is, it is hydrophobic. PCL membranes are expected to retain their mechanical entirety as PCL for many years before they fully degrade [78].

 doi:10.20944/preprints202309.0709.v1



Huang et al. fabricated a new clay-enhanced PCL/chitosan/curcumin (PCL/Clay/CS/Cur) composite film and measurements with instrumental techniques revealed successful clay dispersion. The morphology of clay-fortified Cur-loading films was discovered to be porous spongy with discrete structures. The tensile strength was found to be significantly increased by the addition of nanoclay, going from 1.94 to 11.81 MPa. Additionally, compared to membranes without clay, the drug-loading films with clay showed better controlled-release profiles of curcumin. Skin disinfection tests and SEM measurements revealed that almost no bacteria were present on the wound covered with a PCL/Clay/CS/Cur film, proving that the film was successful in preventing bacterial (Staphylococcus aureus) infection [79].

Karimian et al. synthesized the PCL/cellulose nanofiber nanocomposite containing $ZrO_2$ nanoparticles (PCL/CNF/$ZrO_2$) in three different $ZrO_2$ amounts (0.5, 1, 2%). TGA, DTA, DSC results showed that the nanocomposite has more thermally stable ($T_d$ changed from 367.69 to 377.83 °C for 1% $ZrO_2$) and strength properties than PCL. This nanocomposite was used for wound dressing bandage and exhibited moderate to good antimicrobial function opposed to all tested bacterial (S. aureus and E. coli) and fungal strains (C. albicans) with an inhibition zone between 6.5 and 9 mm [80].

Electrospun PCL membranes with an average diameter of 1.02-1.76 μm were created by Ramirez-Cedillo et al. by adding microparticles or nanoparticles like Ag, $TiO_2$, and $Na_2Ti_6O_{13}$. These membranes improved bacterial resistance, cell adhesion, and proliferation. Compared to the membranes of PCL/$TiO_2$ (60.8 °C) and PCL/$Na_2Ti_6O_{13}$ (57.8 °C), the PCL/Ag membrane showed the lowest endothermic peak, indicating the melting point (Tm), at 55.57 °C. Strength of PCL/$TiO_2$ increased from 0.6 MPa to 6.3 MPa compared to PCL without particles. One could argue that the $Na_2Ti_6O_{13}$ electrospun composite is better suited for tissue regeneration processes [81].

PCL composite membranes reinforced with $TiO_2$ nanoparticles (NPs) were produced using two different solvents, acetic acid and a mixture of trichloromethane ($CHCl_3$) and N,N-dimethylformamide (DMF). The PCL/$TiO_2$ membranes prepared with $CHCl_3$-DMF had better surface homogeneity than those prepared with acetic acid, according to experimental measurements of their physicochemical properties. It was discovered that the compound crystallization changed as the $TiO_2$ NPs content increased. Thus, the pore structures of the PCL membranes as well as their physical characteristics, including strength, ductility, surface roughness, and contact angle (80-103°), were affected by the concentration of $TiO_2$ NPs and the solvent's characteristics. The membrane samples developed with acetic acid had the highest roughness values (lateral resolution ~11 μm for acetic acid, 6 μm for $CHCl_3$-DMF solution). Therefore, it can be said that PCL and $TiO_2$ nanoparticles interact well with the $CHCl_3$-DMF solvent [82].

Scaffaro et al. reported a rapid method for designing multi-scale nanohybrid structures (GO-CNT@PCL) that include a 3D fibrous PCL network encircled by graphene oxide (GO) layers that contain carbon nanotube (CNT) brushes with π-π stacking. The process is based on the electrospinning of PCL solutions onto a suspension of GO and CNTs in ethyl alcohol. The hierarchical architecture and nano-patterned surface allow the initial characteristics of PCL, GO, and CNTs to be aggregated into ultra lightweight (99% porosity), but robust (1575% hardness enhancement) and amphiphilic (both hydrophilic and hydrophobic) monoliths. Some physical properties of this nanohybrid material such as surface tension (28.6 mN/m) and electrical conductivity (29.3 μS/cm) were better than pure PCL (27.3 mN/m, 0.7 μS/cm). These nanohybrid monoliths removed MB and MO from aqueous solution in approximately 100% yield [83].

Preprints (www.preprints.org) | NOT PEER-REVIEWED | Posted: 12 September 2023 doi:10.20944/preprints202309.0709.v1



## 6. Applications of PCL Blends/Composites

### *6.1. Pollutant Removal Applications of PCL Blends/Composites*

#### 6.1.1. Dye Removal by PCL Blends

Some polymers, particularly those with efficient functional groups that are insoluble in water, have been employed as adsorption agents for the removing of dyes and heavy metal ions. Polymers' ability to remove pollutants is determined not only by their active functional groups, but also by their structure, surface area, and porosity. Because of its limited adsorption capacity, low mechanical qualities, and water-insoluble hydrophobic features, pure PCL is ineffective as an adsorbent. Because of these poor qualities, polymer blends or composites of PCL have been employed as excellent adsorption agents for the elimination of dyes from aqueous solution in place of pure PCL. Blending a hydrophobic polymer (PCL) with functional polymers such as cellulose, chitin, chitosan, lignin, and alginate at varying ratios is significant for enhancing adsorption active sites and lowering costs. When compared to other polymer classes, polymer nanofibers offer unique features like high water permeability, high porosity and surface area. As a result, converting ε-caprolactone polymers into PCL fibers is another successful approach for dye removal [84].

For instance, Guo et al. fabricated novel composite fiber adsorption materials with different mass ratios consisting of PCL and beta-cyclodextrin-based polymer (PCD) by electrospinning. The fiber materials obtained showed exceptional elective adsorption for MB and 4-aminoazobenzene (AAB) solutions. Addition of a PCD constituent to composite fibers improved the mechanical resistance (breaking stress 3.41 MPa for PCL/(50%)PCD) of membranes and altered the sorption uptake because of the molecular structure of the cavity through host–guest interaction. The specific surface area values rose substantially with increasing of PCD constituent in the composite fibers, reaching 11.5 $m^2/g$ for PCL/(50%)PCD composite fibers (7.50 $m^2/g$ for neat PCL fibers), suggesting the development of additional anchoring sites aiding the subsequent adsorption of dye compounds. The dye removal efficiency reached from 7.44 mg/g to 24.1 mg/g for AAB and from 3.89 mg/g to 11.2 for MB. Because of the excellent stability and selectivity of the adsorption process, the currently produced beta-cyclodextrin-based composite fibers (average diameter of 200–400 nm) have shown potential large-scale uses in dye capture and wastewater remediation [85].

Many investigations are being conducted to find effective and ecologically acceptable techniques of degrading phenols and their derivatives. In order to create novel types of biocatalytic systems capable of removing bisphenol A, an attempt was made to generate PCL-chitosan electrospun materials for tyrosinase immobilization. SEM scans validated the shape of the fibers and enzyme deposition. After enzyme deposition, fiber diameter increased significantly from 344±121 nm to 689±365 nm, demonstrating enzyme adhesion to the fiber surface. The constructed system was used in batch tests including the biodegradation of bisphenol A under different remediation circumstances. Over 80% of the pollutant was eliminated after 120 minutes of processing at temperatures ranging from 15 to 45 degrees Celsius and pH levels ranging from 6 to 9, using solutions containing up to 3 mg/L. After 30 days of storage, the immobilized biomolecule tyrosinase retained around 90% of its original activity (60% for free enzyme) and was still capable of removing more than 80% of bisphenol A even after 10 repeated usages [86].

Chitosan-based nanofibrous membranes for dye adsorption from solution were created using hybrid electrospinning of chitosan (CS) and PCL or PCL-block-poly(ethylene glycol) (PCL-b-PEG or abbreviated with P) amphiphilic copolymers. PEG segments were shown to be capable of controlling the secondary fiber and core-shell structure. The addition of PEG component enhanced the compatibility of PCL and CS, decreased CS loss because of intermolecular hydrogen bonds formed between CS and PCL-b-PEG copolymer, and increased membrane stability. The adsorption studies revealed that the anionic CR dye adsorption process on CS-based membranes fits well with the pseudo-second order and the Langmuir isotherm models. The CS-based membranes (CS/$P_{5K}$, diameter of ~807.89 nm) with a PEG molecular weight of 5 kDa had high reusability, with highest adsorption capacity of 291.55 mg/g computed using the Langmuir model. The CS/$P_{5K}$ removal effectiveness maintained at

 doi:10.20944/preprints202309.0709.v1



90.18% and dropped to 80% after 10 repetitions, demonstrating that the CS/$P_{5K}$ nanofibrous membrane can be reused for dye removal. As a result, CS/PCL/PEG nanofibers appear to be promising membranes for water purification [87].

Amphiphilic PCL-PEG-PCL/Bentonite A2 nanocomposites were synthesized by in situ ROP of $\varepsilon$-CL in the existence of PEG chains, catalyzed by a intercalated Algerian Bentonite tetrabutylammonium hydrogen sulfate (TBHSA) (A1). For this purpose, sodium cations in bentonite were exchanged by tetrabutylammonium cations [$(C_4H_9)_4N^+$]. The XRD and transmission electron microscopy (TEM) measurements revealed that the silicate sheets in the PCL-PEG-PCL/layered silicate nanocomposites were partly exfoliated. The nanocomposite (A2) was employed to efficiently remove MB dye from aqueous medium. As the mass of the nanocomposite rose, so did the dye's adsorption capacity, which reached an ideal value of 0.13 g adsorbent at pH = 6.8. Calculating an adsorption capacity ($q_{max}$) of 600 mg/g within 90 minutes, the Langmuir isotherm provided the best match [88].

Karagöz et al. designed and manufactured electrospun PCL nanofibers (NFs) adjusted with $TiO_2$ and Ag NPs. The as-prepared PCL/$TiO_2$-Ag NFs mats were created using one-step electrospinning and used for three separate applications: (a) reusable surface-enhanced Raman spectroscopy (SERS) substrate for non-qualitative analysis to track pollutants, (b) photocatalyst for organic pollutant degradation, and (c) antibacterial agent to kill bacteria. For the detection of MB dye, PCL/$TiO_2$-Ag NFs performed to be a highly efficient SERS platform with a detection limit of 10 nM (MB). The photocatalytic degradation of the probe analytes MB under UV irradiation was completed in less than 180 minutes with degradation efficiency 93-95% using a PCL/$TiO_2$-Ag NFs nanocatalyst [89].

A membrane having a greater hydrophilic nature is predicted to be more fouling resistant. The biodegradable nature of PCL and the antifouling property of $TiO_2$ were combined in a composite and used in the construction of water purification membranes. $TiO_2$ nanoparticles' strong association boosted the stiffness of the supramolecular polymeric chain and improved the thermostability of the composite membranes. Porosity and pore size must also be evaluated to establish the membrane's appropriateness for separation applications. To promote pore development in the membranes, PEG is supplemented to the polymeric solution. The tensile strength of the membranes (2.5 N/$mm^2$) was increased by combining PEG with PCL and including $TiO_2$ nanoparticles. The optimal PEG and $TiO_2$ compositions were 6.24 and 1.0 wt% in PCL-$TiO_2$-PEG membrane, respectively. After of bovine serum albumin filtering, the antifouling property of $TiO_2$ gave rise to roughly 90% flux recovery for the PCL-$TiO_2$-PEG membrane when compared to the PCL-PEG membrane. For membranes in water remediation uses, the PCL-$TiO_2$ combination would be a superior option [90].

Immobilization of particular bacteria onto electrospun nanofiber webs of PCL was used to create innovative biocomposite materials. After adequate numbers of bacteria were immobilized on electrospun nanofiber webs, equivalent web samples were used to evaluate their ability to remove the Setazol Blue BRF-X dye. Both PCL/bacteria and PLA/bacteria webs eliminated the Setazol Blue BRF-X dye within 48 hours at each dose investigated (50, 100, and 200 mg/L), and their removal efficiency (87.88% and 89.57% for 50 $mgL^{-1}$ of dye concentration) were extremely similar to free bacterial cells. The samples' $Q_{eq}$ values were in the same order: 119.56 $mgg^{-1}$ for free bacteria, 109.75 $mgg^{-1}$ for PCL/bacteria web samples, and 112.15 $mgg^{-1}$ for PLA/bacteria web samples. The bacteria immobilized webs were then evaluated for 5 reuses at starting dye concentration of 100 mg/L and found at the end of the test to be potentially reusable (removal capacity of PCL/bacteria:95.36%), with higher bacterial count immobilization and faster removal of dyes. Overall, their findings indicate that electrospun nanofiber webs are viable platforms for bacterial integration and that webs immobilized with bacteria can be employed as starting inoculants for the removal of textile dyes from aqueous medium [91].

Polydopamine (PDA) nanoparticles have a high adsorption capacity and can be utilized as an adsorbent. On the other hand, nano-sized PDA adsorbents are prone to aggregation and so have severe limitations in the adsorption field. To address this issue, Wang et al. produced the PCL/PEO copolymer by electrospinning and blended it with PDA. They discovered that modifying the surface and porosity of the produced nanofibers enhanced their adsorption capability. The PCL/PEO@PDA composite illustrated a high number of active sites for MB and MO adsorption. It is important to note that the PCL/PEO@PDA-45 composite as an adsorbent showed a better matched adsorption capacity

Preprints (www.preprints.org) | NOT PEER-REVIEWED | Posted: 12 September 2023 doi:10.20944/preprints202309.0709.v1



for the anionic dye MO (60.22 $mgg^{-1}$) than that of the cationic dye MB (14.85 $mgg^{-1}$). Furthermore, the PCL/PEO@PDA blends were reusable numerous times and performed well as adsorbents. The removal effectiveness of the PCL/PEO@PDA adsorbent on MO dye reduced from 99% to 93% after eight reuses, confirming the adsorbent's outstanding stability and recyclability [92].

Self-assembly nanohybrid structures GO@PCL, CNT@PCL, and GO-CNT@PCL produced by wet electrospinning-aided with a 3-dimensional fibrous PCL network surrounded by graphene oxide (GO) layers on which carbon nanotube (CNT) brushes were stuck. They studied the influence of surface chemistry on the sorption ability of fluffy scaffolds nanohybrid materials towards water soluble organic dyes such as MB and MO. Given that such a cationic MB dye may interact with aromatic and oxygenated areas of composites, all of the compounds perform quite well in terms of MB removal. GO-CNT@PCL outperformed the other nanohybrid samples, with a sorption capacity of 400 $mgg^{-1}$ and an elimination efficiency of almost 100%. In the instance of MO removal, GO-CNT@PCL demonstrated 100% effectiveness with more than 80 $mgg^{-1}$ adsorption in 6 h, likely due to the combination of wettability by GO and the amount of active sites by CNTs [93].

Three PEG/PCL copolymers were prepared with various topologies but the same mol ratio of PEG to PCL. Different techniques were used to characterize these compounds, which included di-block (Di-PEG-PCL), tri-block (Tri-PEG-PCL), and multi-block (Multi-PEG-PCL) copolymers. The influence of topology on the efficiency of MB removal from aqueous medium was researched. The multi-block copolymer outperforms other topologies in terms of adsorption efficiency. The regression coefficient data showed that the Freundlich isotherm ($R^2$= 0.9840) accurately describes the MB adsorption by copolymers [94].

### 6.1.2. Dye Removal by PCL/Metal Oxide Composites

Metal oxides are added to PCL to improve dyeability, thermal stability, adhesion, and other properties. Because it is miscible with a wide range of metal oxides, flexible, biocompatible, and mechanically suitable, it has the exceptional ability to enhance the characteristics of other materials, which results in a wide range of applications.

The electrospinning method was used to create high surface area porous PCL membranes containing $Fe_3O_4$ nanoparticles. In the existence of $H_2O_2$ and UV light, they were tested as degradation catalysts in Fenton reactions to breakdown cationic MB dye. The results showed that the fiber catalyst system (fiber diameter: 713 ± 139 nm for 15% PCL) performed well in terms of MB removal (99% MB) and was functional after 6 cycles (96% MB). PCL membranes may interact strongly with organic compounds because to their hydrophobic surfaces. The excellent catalytic properties of the composites are attributable to the synergy of the porous surface (pore size spans from 2.43 to 6.56 μm) and the implanted $Fe_3O_4$ nanoparticles. It also has the benefit of being environmentally safe and readily separated without the use of an external magnetic field [95].

PCL nanofibrous membranes integrated with hydroxyapatite (HAP) adjusted with varying concentrations of Cu(II) ions were created. A variety of spectrometric, microscopic, and surface science methods were used to describe the architectures, morphologies, and surface roughness's of the built (Cu-HAP@PCL) membranes. Examination of the surface morphology showed that these membranes present as web fibers with different diameters ranging from 0.45–1.5, 0.45–1.21, 0.21–1.5, 0.3–1.1 to 0.2–0.9 μm; however, the average roughness increased exponentially with increasing Cu(II) ion content. The maximum degradations of MB dye were achieved after 70 minutes of visible light irradiation utilizing the constructed Cu-HAP@PCL membranes, with values of 88.6%, 89.4%, 91.0%, 91.1%, and 94.3%. The degradation mechanism can be summarized by the following reactions.

$$[Cu_xCa_{1-x}(PO_4)_6(OH)_2] + h\nu \rightarrow e^-(CB) + h^+(VB) \quad (5)$$

$$[Cu_xCa_{1-x}(PO_4)_6(OH)_2] + H_2O + 2e^- \rightarrow 2OH^- + Cu \quad (6)$$

$$e^- + O_2 \rightarrow O_2^{*-} \quad (7)$$

$$e^- + O_2^{*-} + 2H^+ \rightarrow H_2O_2 \quad (8)$$

Preprints (www.preprints.org) | NOT PEER-REVIEWED | Posted: 12 September 2023 doi:10.20944/preprints202309.0709.v1



$$2e^- + HO_2^{*-} + H^+ \rightarrow OH^* + OH^- \quad (9)$$

$$MB + OH^* \rightarrow MB(degenerated) + CO_2 + H_2O \quad (10)$$

Hydroxyl ions (OH*) and superoxide scavengers ($O_2^{*-}$) are the most efficient ions in the destruction of MB dye. Because these ions have a strong chemical activity while interacting with MB molecules, small fragments of molecules may be formed [96].

Elias et al. investigated the efficiency of a PCL-organically modified montmorillonite clay (Cloisite 10A) nanocomposite membrane in the removal and degradation of rhodamine B from aqueous systems under VIS light (50 W). A nanocomposite containing 9 by weight of Cloisite 10A effectively converts rhodamine B into environmentally friendly products in less than 3 hours. C10A's adsorptivity and -OH groups on the surface promote electron-hole pair separation and improve photocatalytic activity [97].

The feasibility of immobilizing $TiO_2$ nanoparticles (NPs) on PCL beads and foams for the photodegradation of textile dyes in wastewater is discussed in this work. PCL foams were created by treating PCL beads in supercritical carbon dioxide in an ecologically friendly manner. Within 24 hours of exposure to sun-like illumination, PCL beads and foams filled with $TiO_2$ NPs were utilized as photocatalysts to degrade the textile dyes C.I. acid orange 7 and C.I. basic yellow 28 from aqueous solutions. Unlike the PCL beads, the PCL foams completely discolored the dye solution after 24 hours of illumination. PCL foams also had exceptional buoyancy that lasted longer than four weeks. Furthermore, their photocatalytic activity was sustained after three cycles of photodegradation, demonstrating that the buoyant photocatalyst outperformed the non-buoyant PCL beads in terms of photocatalytic activity. As a result, the PCL foams with immobilized $TiO_2$ nanoparticles have high photocatalytic activity and maintained floatability, making them a feasible choice for practical usage as a floating photocatalyst in textile industry wastewater management [98].

Geravand and his colleague [99] developed a biodegradable membrane made of PCL/MXene nanosheets ($Ti_3C_2(OH)_2$). Using hydrophilic MXene as the nanofiller resulted in significant improvements in biodegradability, water permeability, and antifouling characteristics. The findings demonstrated that the PCL membrane combined with 4 wt% MXene displayed the maximum hydrophilicity and pure water permeance (PWP), which were nearly four times higher than the neat PCL membrane (5.99 vs 1.43 $L/m^2.h.bar$). Furthermore, the membrane containing 1% MXene exhibited 98.92% rejection of crystal violet ([CV]=50 ppm). All three mechanical features improved with rising the MXene concentration up to 3wt% (elastic modulus from 19.87±0.07 to 36.61±0.52 MPa, tensile strength from 5.14±0.27 to 10.51±0.33 MPa, and elongation at break from 316±6 to 359±7%), however they declined with a continual rise in MXene concentration. The mechanical performance of membranes is affected by a variety of parameters, including MX distribution uniformity, polymer aggregation, and augmented membrane porosity [99].

As photocatalytic materials, neat $TiO_2$ nanoparticles ($TiO_2$ NPs) have limited reusability. To achieve effective photocatalysis, certain high surface area supports are added to the $TiO_2$ loading. Porous electrospun PCL fiber mats were utilized in the study to support the capacity and dispersion of $TiO_2$. The porous PCL mats can provide a broad contact surface area for excellent $TiO_2$ photocatalytic activity. Furthermore, the inclusion of rectorite (REC) might lower fiber diameters, induce stabilization of the anatase phase, and increase specific surface area, which could be favorable to photocatalysis. More notably, REC improved the performance of porous PCL/$TiO_2$ mats, resulting in high photocatalytic degradation. The findings suggested that porous PCL/$TiO_2$/REC mats might be good photocatalysts for the degradation of organic dyes like Rhodamine B. After 3 hours, the crimson solution turned translucent while the mats became red. At the end of the experiment, the photocatalytic activity of $TiO_2$ NPs and fibrous mats all achieved 98%. In the first 45 minutes, the photocatalytic effectiveness of PCL/$TiO_2$/REC mats was greater than that of neat $TiO_2$ NPs, confirming that REC expedited the photocatalytic process [100].

The solution casting approach to create $TiO_2$ nanoparticles embedded polymer films from two biodegradable polymers such as cellulose acetate (CA) and PCL was used. The photo-degradation rate rose with rising content of $TiO_2$ NPs in CA and PCL films. $TiO_2$-PCL films had the highest

 doi:10.20944/preprints202309.0709.v1



photocatalytic efficiency of the two types of polymer materials tested. After 3 hours of UV-A light exposure, PCL film combined with 5% $TiO_2$ had the greatest MB degradation rate (72%), followed by 5% CA film, with 53% dye degradation. As a result of the significant quantity of NPs around the pores and cracks on the film, the porous structure of $TiO_2$ in PCL-$TiO_2$ film could produce high MB degradation [101].

Solution casting was used to create the PCL and $Fe_2O_3$/PCL nanocomposites sheets/films. The morphological analysis revealed that the $Fe_2O_3$ nanoparticles (250 nm) were well disseminated and lodged inside the PCL matrix. The thermal stability of $Fe_2O_3$/PCL was poorer than that of pure PCL, which might be attributed to the activity of $Fe_2O_3$ as a catalyst in the thermal degradation of PCL. According to the DSC investigations, the crystallization temperature of the $Fe_2O_3$/PCL was somewhat higher than that of pure PCL. The polarized optical microscopy studies revealed that the size of $Fe_2O_3$/PCL spherulites was less than that of pure PCL. The UV-Vis spectra demonstrate that as the irradiation period and the number of $Fe_2O_3$ nanoparticles in the nanocomposites increase, so did the photodegradation of rhodamine B (RhB) dye. Within 2 and 10 hours, pure PCL photodegraded between 24 and 72% of the RhB dye, while $Fe_2O_3$ (6 wt%)/PCL composites degraded around 72 and 98% of the dye, respectively [102].

A simple hydrothermal approach was used to create hydroxyapatite (HAP) nanorods that were hydrophobically modified using lauric acid (LA). Pickering emulsion template technique was used to load HAP compound modified by LA (RHAP) and magnetite (m, $Fe_3O_4$) NPs as emulsifiers on PCL microspheres. The structure, constituents, and morphology of synthesized pure HAP nanorods (hydrophilic, water contact angle 11.7°) and m-RHAP-PCL microspheres (hydrophobic, water contact angle 111.3°) were analyzed by XRD, SEM, FTIR, and TGA. MG was used as a model dye to study the adsorption capability of m-RHAP-PCL microspheres. The highest adsorption capacity ($q_{max}$) of m-RHAP-PCL was 609 $mgg^{-1}$, and its relative adsorption performance was greater than that of pure HAP, showing that it has better MG adsorption potential. The values of $R_L$ (from 0.157 to 0.263, which were much smaller than 1) and 1/n (0.204-0.290, which were less than 0.5) suggested that the adsorption process had occurred on its own. Moreover, the adsorbent recovers easily in magnetic fields and its ability to remove MG remains unchanged over four cycles, demonstrating the reusable nature and stability of the m-RHAP-PCL adsorbent for MG sorption [103].

A chitosan/PCL-block poly(ethylene glycol)/$SiO_2$ aerogel@polydopamine (CS/PCL-b-PEG/SA@PDA) membrane was developed for the adsorption and removal of Congo red (CR) dye. Using simultaneous electrospinning electrospray technology, $SiO_2$ aerogel with nanoporous network architecture was immobilized into multicomponent polymer fibers, followed by PDA modification. The composite adsorbent exhibited a highest CR adsorption capacity of 598.8 $mgg^{-1}$ and showed remarkable reusability. Because of the significant amount of $NH_2$, $COO^-$, and OH groups in their structures and amphiphilic characteristics, CS and PCL-b-PEG were chosen as adsorbent template substances in this research [104].

A mat of graphene oxide (GO) nanosheets was employed to dope fine powder of magnetite nanoparticles (MNPs) with varying amounts of copper ions (Cu(II)). These compositions ($Cu_xFe_{3-x}O_4$/GO) were fully integrated into PCL electrospun nanofibrous membranes. The morphological characteristics of the membranes revealed that diameters were varied with Cu(II) ions variation, starting at 0.35-1.06 μm and 1.8-3.9 μm without Cu, being 0.19-0.45 μm and 0.75-1.42 μm for the greatest contribution of Cu, while GO scattered grains of 0.56-1.5 μm were observed. The toughness at the highest additional dopant was 4.69 ± 0.29 $MJ/m^3$, while the tensile strength was adjusted to around 8.96 ± 0.45 MPa. These nanofiber membranes' ability to capture MB dye from aqueous medium was also tested. The created nanofiber membrane could absorb 95.1% of the MB after 36 min of contact time, and the composition was still stable after 5 removals with a performance of about 90.1% for the 0.8Cu-MNPs-GO@PCL [105].

Electrospinning technology was used to create high surface area porous PCL membranes with $Fe_3O_4$ NPs. SEM, XRD, IR spectroscopy, magnetometry, and strain-stress curves were used to investigate the morphology, chemical composition, magnetic and mechanical features. In the presence of $H_2O_2$ and UV light, they were tested as catalysts in Fenton reactions to deteriorate MB. The results

Preprints (www.preprints.org) | NOT PEER-REVIEWED | Posted: 12 September 2023 doi:10.20944/preprints202309.0709.v1



showed that the fibrous catalyst system performed well in terms of MB removal (99% MB) and was usable after 6 cycles (96% MB). The composites' outstanding catalytic properties are caused by the interaction of embedded $Fe_3O_4$ NPs with the porous surface. It also has the advantage of being environmentally friendly and easily separated without the use of an outside magnetic field [106].

Ring-opening polymerization was used to create a PCL/$Fe_3O_4$ magnetic nanocomposite (PCL/$Fe_3O_4$ MNC) in this research. Then, as a new adsorbent, PCL/$Fe_3O_4$ MNC was utilized to capture remazol brilliant violet 5R (RBV 5R) from aqueous solution. The response surface methodology (RSM) was employed to maximize the adsorption procedure and define the optimum conditions. At a contact time of 168 minutes, a PCL/$Fe_3O_4$ MNC amount of 0.40 g and an RBV 5R concentration of 7.18 $mgL^{-1}$, 95.40% RBV 5R removal was obtained. ATR tests revealed that the chemical bonding in PCL/$Fe_3O_4$ MNC did not change significantly before and after the adsorption method [107].

PCL composite was used not only for dye removal but also for oil separation. By incorporating $SiO_2$ aerogel, exceptional superhydrophobic PCL membranes with an alternating hierarchical micro-nanometer structure were created. When the $SiO_2$ aerogel content in the PCL membrane was 0.5% (PCL/$SiO_2$-a0.5), the maximum water contact angle (WCA) of 166.8±1.5° was acquired, which was greater than other published polymer-based membranes. The surface energy of the PCL membrane was reduced by $SiO_2$ aerogel. The internal structure of the PCL/$SiO_2$-a0.5 membrane, which was made up of micro-nano spheres and fibers, increased the porosity of the membrane, allowing for more adsorption area for water-in-oil separation. In the meantime, the PCL/$SiO_2$-a0.5 membrane demonstrated exceptional chemical stability, self-cleaning ability, and reusability [108].

Uzunok and Sönmez improved the hydrophobicity of PCL by incorporating different silane-based cross-linkers such as tris [3-(trimethoxysilyl)propyl] isocyanurate, tetraethyl orthosilicate, and 1,8-bis(triethoxysilyl)octane for the removal of oil from aqueous system. The obtained sorbents showed high and quick absorption properties in the range of 5450-51000 $mg.g^{-1}$. After 10 cycles of oil sorption, the sorbents demonstrated high oil sorption capacity and reusability without any loss [109].

PCL blends/composites have an important place not only in dye and heavy metal removal, but also in oil cleaning. The use of oil-soaked adsorbents in the recovery and clean-up of oil spills is gaining importance day by day. Recently, magnetic nanoparticle (MNP)-based absorbers have attracted interest as a new method both to treat oil spills and to reduce the amount of labor required. Eom et al. performed the synthesis of MNP embedded PCL adsorbent, which can be easily collected under magnetic field, has oleophilic and environmentally friendly properties. MNP embedded PCL adsorbent (MNP/PCL) exhibited perfect Arabian light (AL) crude oil absorption capacity (45.7 g/g) and reduced the absorption time of oil-immersed sorbent because of its electrospun structure. In the future, such sorbents may be applicable in large scale oil spill projects [110].

### 6.1.3. Heavy Metal Removal by PCL Composites/Blends

PCL is one of the promising compounds for manufacturing biocompatible membranes due to its outstanding structure and superior mechanical and physical features. PCL nanocomposites have also found usage in removing of heavy metal ions from aqueous system. Bio-nanocomposites CD-PCL-$TiO_2$ was utilized as an adsorbent material in removing of Pb(II) ions from wastewater after a two-step process of sol gel synthesis of $TiO_2$ particles and polymer solution blending. The highest removal of Pb(II) ions was 98% at pH 9.7, concentration 10 ppm, and dosage of 0.005 g. This method has a significant advantage in that it does not introduce any secondary pollutants into the treated water [111].

Liakos et al. mixed the solutions of 8.42% by weight PCL in dichloromethane with sodium alginate (SA) (5, 10, 15, 20, 25 or 30% by weight based on PCL) and the resulting films were placed in a heat extruder to form PCL/SA filaments.

The goal of this study is to develop new composite filaments relying on thermoplastic PCL polymers, which are water resistant and compatible with 3D printing technologies, to be used in environmental remediation by removing toxic metal ions. The interplay and stability of SA with PCL was because of the creation of hydrogen bonds between the former's hydroxyl groups and the latter's carbonyl groups. The resulting composite filaments with 30%SA had a highest adsorption capacity

Preprints (www.preprints.org) | NOT PEER-REVIEWED | Posted: 12 September 2023 doi:10.20944/preprints202309.0709.v1



of around 90 $mgg^{-1}$ for heavy metals such as copper(II) ions in aqueous system [112]. It was shown that the pure PCL filament did not absorb any Cu ions and all the SA-containing filaments showed Cu ions adsorption capabilities.

Electrospinning was used to create nanostructured membranes of cellulose acetate (CA) with varying PCL loadings (0%, 10%, 20%, and 30%) in removing of $Pb^{2+}$ ions from aqueous medium. Using instrumental techniques revealed that the introduction of PCL into CA resulted in a finer fiber radius, increasing the membrane's surface area and thus increasing the number of adsorption sites. According to the findings, $Pb^{2+}$ ion adsorption capacity was increased from 43.96 $mgg^{-1}$ of pristine CA membrane to 70.50 $mgg^{-1}$ of CA/10%PCL filled membrane. Furthermore, the findings of this experiment agreed best with the pseudo second-order kinetics and Freundlich isotherm, both of which accurately described the adsorption process [113].

Coaxial electrospinning was used to create core-shell-structured CA-PCL/CS nanofibers with outstanding hexavalent chromium (Cr(VI)) removal performance. In an acidic environment, the influence of the core/shell ratio on the adsorption ability was investigated. The findings demonstrated that when compared to the CS powder adsorbent, all core-shell-structured fibrous demonstrated improved adsorption and durability. CA-PCL/CS fibrous with a core/shell ratio of 0.442 absorbed 126 $mgg^{-1}$ of Cr(VI) ions at RT. Adsorption kinetics showed that chemisorption was the rate-limiting step due to significant electron transfer, sharing or exchange between CA-PCL/CS nanofibers and Cr(VI) ions [114].

Benhacine et al. combined PCL with silver montmorillonite (Ag-MMT) to produce nanocomposite membranes. SEM analysis revealed that the synthesized membranes had homogeneous sponge microstructures. Gradual incorporation of nanoparticles (2, 3, and 5 wt%) into the PCL matrix resulted in a significant increase in membrane thickness. The authors of the current study administered the treatment to actual wastewater samples and documented a decrease in the concentrations of nitrates by 15.12% and sulphates by 45.61%, along with significant reductions in the levels of Pb, Zn, and Cd, by 41.38%, 53.57%, and 61.11%, respectively [115].

Irandoost et al. prepared nanofiber nanocomposite of PCL adsorbent modified by binary fillers such as nanoclay and zeolite clinoptilolite NPs to improve the adsorption properties. Lead removal studies have shown that each component in the nanofibrous adsorbent has a synergistic effect on the Pb(II) adsorption capacity (19.92 mg/g). In thermodynamic studies, negative $\Delta G$ values (between -0.173 and -3.003 kj/mol) indicated spontaneous Pb(II) adsorption in all temperatures and concentrations [116].

Using the electro-spinning method, a composite membrane based on PCL/cellulose nanofibers (CNF) with various ratios was fabricated with the goal of developing organic membranes with excellent mechanical features for removing impurities from tap water. The resulting green and environmentally friendly membranes exhibited structures containing nanometric porosity. Water quality variables evaluated after filtration with the PCL/CNF membranes revealed 100% turbidity removal, 100% conductivity and heavy metal removal ranging from 75% to 99% for iron and chromium [117].

#### 6.1.4. Adsorption Mechanism of Dyes/Metal Ions onto PCL Composites/Blends

Water-insoluble homo-PCL polymers are not very effective against environmental pollution such as heavy metal ions and dyes due to their low adsorption efficiency, low pore volumes, low pore sizes and high hydrophobic properties. Instead, PCL blends/composites are preferred as effective adsorbents for removing dyes and metal ions from an aqueous medium [118,119]. The blend of a polymer including functional groups with a hydrophilic polymer like cellulose, chitosan, and chitin in various ratios is crucial for enhancing hydrophilicity, raising adsorption active sites, and decreasing cost. Understanding the adsorption mechanism of dyes or heavy metal ions on PCL adsorbents is critical for optimizing the adsorption method and improving the efficiency of PCL nanofibers in dye removal. The adsorption of dyes or metal ions on the surface of nanofiber materials is controlled by solution conditions (such as pH and temperature), nanofiber nature (like porosity, area of surface, functional moieties, and surface morphology), and dye nature (like neutral, cationic, and anionic forms, and molecular size of dyes) [120,121]. The adsorption mechanism may be unclear due to the

 doi:10.20944/preprints202309.0709.v1



variety of factors influencing dyes or metal ions adsorption onto the surface of nanofibrous. It is essential to carry out isotherm, kinetic, thermodynamic, and spectroscopic studies, in addition to looking at the impact of pH in order to gain a clear and comprehensive understanding of the adsorption mechanism. According to various studies [122,123,124], dyes or metal ions removal from effluents using pure PCL, PCL blends, and PCL composites are most likely accomplished through hydrogen bonding, van der Waals (VDW) forces, stacking, hydrophobic interactions, electrostatic interactions, and pore filling. The interactions are influenced by the type of functional moieties on the surface of PCL nanofibrous, their morphology, and the type of filler added to the nanofibrous. These interactions, which operate concurrently to varying degrees, can be utilized to explain the adsorption mechanism of dyes and metal ions [84,125,126,127].

Draoua et al. investigated the MB dye removal adsorption performance of a PCL-PEG-PCL/Bentonite nanocomposite [88]. They came to the conclusion that the sorption mechanism is dependent on the hydrophobic interaction between the dye and the copolymer's hydrophobic block (PCL), as well as the electrostatic interaction between the surface (the SiO- and AlO-) and the edge moieties of bentonite and the dye's sulfonic group.

Alrafai et al. [96] studied the degradation mechanism of MB on the surface of PCL nanofiber membranes associated with hydroxyapatite (HAP) doped with varying quantities of Cu(II) ions (Cu–HAP@PCL). The degradation efficiency of MB dye on the fabricated Cu–HAP@PCL membranes indicated that the maximum degradation of 94.3% was accomplished after 70 min exposure to visible light. They discovered that the degradation efficiency is primarily increased by increasing the Cu contribution and the lengthening of the irradiation time [96].

Chen et al., for example, used FTIR and XPS techniques to investigate the adsorption mechanism of CR dye on the surface of CS/PCL-b-PEG/SA@PDA membrane. They came to the conclusion that dye adsorption was accomplished through a combination of interactions like hydrophobic, hydrogen bond interactions (between the adsorbent's amine and hydroxyl groups and the CR's sulfonate groups), and adsorption space on porous membrane [104].

Pekdemir et al. suggested that there are two possible mechanisms for dye adsorption on the adsorbent surface. They are chemical and physical interactions between the dye compound (RBV-5R) and the polymer (PCL/$Fe_3O_4$) nanocomposite. The hydrogen bonding, π–π interactions, and VDW interactions between the adsorbing agent and the dye compound are thought to control the adsorption rate in the model [107].

Hussain et al. crosslinked tannin (TA)-reinforced 3-aminopropyltriethoxysilane (APTES) with PCL fabricated via electrospinning and investigated colorimetric performance of membrane for $Fe^{2+/3+}$ ions. They discovered that Fe ions bind to the crosslinked composite membrane due to FeTA complexation to form PCL-FeTA-APTES. According to the results of adsorption filtration, PCL-FeTA-APTES membrane is reusable and has higher MB dye adsorption (32.04 $mgg^{-1}$) than PCL-TA-APTES membrane (14.96 $mgg^{-1}$). This finding showed that the adsorption mechanism is influenced by high adsorption sites on the PCL-FeTA-APTES membrane, which allows the weak π-π interaction and electrostatic attraction between the cationic dye compounds and anionic adsorption sites of the membrane [128]. Figure 5 outlines adsorption mechanisms of heavy metal ions and dyes onto PCL-blends and PCL-composites.

Preprints (www.preprints.org) | NOT PEER-REVIEWED | Posted: 12 September 2023 doi:10.20944/preprints202309.0709.v1



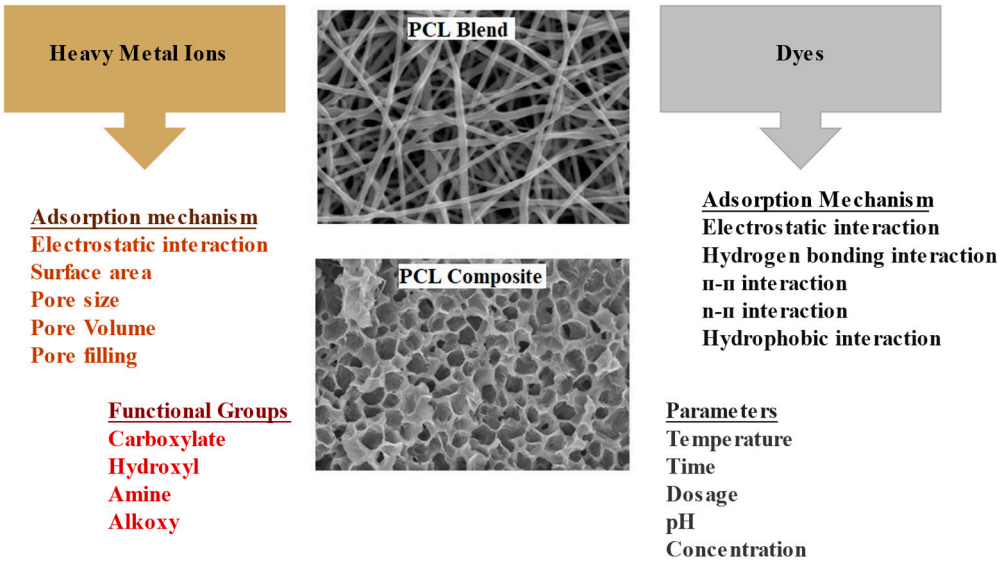


**Figure 5.** Adsorption mechanisms of heavy metal ions and dyes onto surface of PCL, PCL-blends, PCL-composites [84,120,121,126,127].

Lee et al. prepared coffee/PCL composite filters from coffee grounds and PCL and utilized them to eliminate Cu(II) ions from aqueous system [129]. They discovered that for 50 and 100 M Cu(II) ions, the removal efficiency of coffee/PCL composites was 96.6% for 4 hours ($q_{max}$=25.91 mg/g). All samples' adsorption processes exhibited both monolayer and multilayer adsorption characteristics. The adsorption of Cu(II) ions was attributed to the strong binding or interaction between adsorbent and adsorbate.

In the study of Ramírez-Rodríguez et al., the hybrid membrane of PCL-whey protein isolate (PCL-WPI) adsorbed significant amount of Cr in just under 60 minutes because of abundance of adsorption sites on the adsorbing agent surface. However, the adsorption of Cr dropped significantly with time because of occupation of the active sites of the membrane and adsorption equilibrium was reached after 3.5 h [130].

The dynamic elimination of arsenic from aqueous medium with an adsorption membrane composed of an iron-intercalated montmorillonite-filled PCL matrix (Fe-MMT/PCL) was performed by Pena et al. [131]. According to parametric studies, longer breakthrough times are associated with a low flow rate (20 $mLmin^{-1}$), a low starting inlet concentration (2 ppm), and a thick nanofiber membrane (0.75 mm).

Composite membranes with functionalized fillers are being investigated for selecting adsorption. Carbon Quantum Dots-Polyacrylonitrile(PAN)/PCL nanocomposite membranes are prepared by electrospinning and are designed for Cu(II) adsorption. The maximum adsorption capacity of a nanofiber mat with respect to contact time was 63.45 $mgg^{-1}$, with a highest adsorption efficiency of 90.74%. CQD in PAN and PAN/PCL membrane magnified the fiber size distribution from 50-100 nm to 150-250 nm, increasing the hydrophilicity of the PAN/PCL membrane. The physical adsorption method, which involves VDW forces and hydrogen bonds between adsorbent and adsorbate, governs the adsorption behavior [132].

The surface chemistry of the cellulose acetate (CA)/PCL electrospun fibers immobilized wit the novel mercury-favored organic dye (NF06) sensor was discovered to effectively facilitate the sensor's fluorescence resonance energy transfer (FRET). Following Hg(II) chelation, both mobile and immobilized NF06 carried out FRET via a ring-open mechanism. Since the thiorhodamine-6 G acceptor stayed in a cyclic spirolactam in the lack of Hg(II), the FRET process was found to inhibit. However, due to the favorable electrostatic interactions between Hg(II) and the N- and S-atoms of NF06, an

Preprints (www.preprints.org) | NOT PEER-REVIEWED | Posted: 12 September 2023 doi:10.20944/preprints202309.0709.v1



NF06:Hg(II) complex could easily form once Hg(II) was present. Consequently, the thio-R6 GH evolved from a ring-closed to a ring-opened spirolactam version [133].

Bernhardt et al. [134] studied the ability of PLLA to enhance the adsorption capacity of PCL in removing Rose Bengal from aqueous system. Solid samples of the PLLA-PCL-PLLA system were discovered to quickly eliminate over 90% of Rose Bengal from aqueous medium, resulting in the fully vanishing of the distinctive pink color. Rose Bengal was also effectively removed from water by solutions of the copolymers in $CH_2Cl_2$. Large inclusion formation constant ($K_i$) values ranging from $1.0x10^5$ to $7.9\ x10^5\ M^{-1}$ were obtained, and an average adsorption capacity of $6.2x10^{-7}$ mol/g polymer was determined. The increased adsorption capacity was attributed the hydrophilicity of co-polymer because of the PLLA [134].

As a result, it was found that the formation of novel functional groups that increase the number of adsorption sites on the nanofibrous surface, increases the adsorption capacity of polymer nanofibrous when they are combined with one or more polymeric materials. Additionally, for describing the adsorption process of cationic, anionic dyes and heavy metal ions on the surface of blends and composites of PCL, the Langmuir and PSO models were the best isotherm and kinetic models. Tables 3 and 4 give some examples of PCL blends and composites for removing dyes and toxic metal ions from aqueous system, but it is not easy to compare them. Because the results vary greatly depending on experimental conditions like temperature, initial concentration, adsorbent amount, contact time, and pH. As a result, PCL blends and composites with high adsorption capacity were prepared and studied.

**Table 3.**

| PCL-Blends/Composites | Time | Dyes | Adsorption Capacity, $mg.g^{-1}$ | Ref. |
|---|---|---|---|---|
| PCL/(50%)PCD | 2h | MB | 11.2 | [85] |
| CS/$P_{5K}$ Nanofibrous Membranes | 2h | CR | 291.55 | [87] |
| PCL-PEG-PCL/Bentonite A2 | 1.5h | MB | 600 | [88] |
| Bacteria/PCL Webs | 48h | Setazol Blue BRF-X | 109.75 | [91] |
| PCL/PEO@PDA-45 | 45h | MO | 60.22 | [92] |
| GO-CNT@PCL | 6h | MO | 80 | [93] |
| Tri-PEG-PCL | 2h | MB | 193.51 | [94] |
| Multi-PEG-PCL | 2h | MB | 256.01 | [94] |
| m-RHAp-PCL Microspheres | 55h | MG | 609.76 | [103] |
| CS/PCL-b-PEG/SA@PDA-24 | 24h | CR | 598.8 | [104] |
| PCL-FeTA-APTES | - | MB | 32.04 | [128] |
| PCL-BIX80 | 2h | MB | 79 | [135] |
| PCL-BIX80 | 2h | BG | 254 | [135] |
| PCL/PEI/TTL | 8h | MG | 36.5 | [136] |

**Table 4.**

| PCL-Blends/Composites | Time | Heavy Metal Ions | Adsorption Capacity, $mg.g^{-1}$ | Ref. |
|---|---|---|---|---|
| PCL/30%SA Filaments | 30 days | Cu(II) | 93.3 | [112] |
| CA/10%PCL Membrane | 6h | Pb(II) | 70.50 | [113] |
| CA–PCL/CS | ? | Cr(VI) | 126 | [114] |

 doi:10.20944/preprints202309.0709.v1



| | | | | |
|---|---|---|---|---|
| PCL/Clay/Zeolite | 2h | Pb(II) | 19.92 | [116] |
| Coffee/PCL | 4h | Cu(II) | 25.91 | [129] |
| CQD/PAN/PCL | ? | Cu(II) | 63.45 | [132] |
| 10%PCL/5%Clay Fiber | 72h | Cd(II), Cr(III), Pb(II) | 29.59, 27.23, 32.88 | [137] |
| PCL-CuHCF | 40 min | Cs(I), Co(II) | 178.7, 85.06 | [138] |
| PCL/Mg micromotor | 3 min | Ag(I) | 0.635 | [139] |
| Fe-MMt/PCL | 6h | Hg(II) | 14.25 | [140] |
| CMKC-coated PCL scaffolds | 1 min | Ca(II) | 2.186 | [141] |
| TPCL | 30 min | Pb(II), Cd(II) | 10.27,5.81 | [142] |

*6.2. Other uses like biomedical applications*

Similar blends or composites of PCL have been used not only in dye and heavy metal removal, but also in tissue engineering, drug release, wound healing and other fields. PCL has many desirable properties for use as a biomaterial. Despite its low biocompatibility, its rubbery properties, tunable biodegradability, and ease of formation into blends, composites, and copolymers make it a desirable material for utilization as a supporting device, particularly for hard tissue, a good scaffold material for tissue engineering, and a desirable material for surgical sutures and micro/nano vesicles for drug delivery [73]. Its surface roughness and hydrophilic adjustability also supplies preferred surfaces and interfacial features for the tissue. Degradation is affected by molecular weight, shape, residual monomer content, autocatalysis, and other factors. Generally, it takes 2-3 years for PCL to completely degrade in the tissue fluid, which is constantly changing in the biological environment. The degradation of materials utilized in the manufacture of scaffolds for tissue engineering implementations is an important property. In tissue engineering, the rate of material degradation is expected to be similar to the rate of tissue regeneration. When degradation is slower than the rate of tissue regeneration, it impedes tissue growth; when it is faster, it causes the linkage between tissue and scaffold to be lost, delaying the healing process [143].

Das et al. described a novel method for producing PCL/chitosan structure including membrane products with double-porosity (macrovoids with interconnected microporous network) by chemically optimizing the solvent-containing and non-solvent phases and using a customized phase transition method. The existence of chitosan in the chitosan/PCL structure improved hydrophilicity significantly. The cytocompatibility of the chitosan/PCL scaffold was also investigated and found nontoxic. In the future, the blend membrane with dual porous morphology can be used for small radius vascular bypass uses. Surface macrovoids (20-90 μm) may be beneficial for three-dimensional cells adhesion and incrementation, while an interconnected microporous spongy network (7-20 μm) is anticipated to transport vital nutrients, oxygen, and growth factors between the macrovoids and the supernatant. All of these findings indicated that the chitosan/PCL nanofibrous structure would be a fantastic system for bone and skin tissue engineering [144].

Antioxidants are essential for the accomplished neural tissue regeneration, and biomaterials with antioxidant action may be beneficial for peripheral nerve repair. To create an antioxidant bioscaffold for nerve regeneration, Wang et al. used solvent-free ROP to create lignin-PCL copolymers. The lignin/PCL copolymers were then combined with PCL and designed into nanofiber scaffolds to support neuron and Schwann cell growth. The inclusion of lignin-PCL improved the mechanical features of PCL nanofibrous while also providing good antioxidant characteristics (up to 98.3±1.9% inhibition of free radicals within 4 h). These findings proposed that nanofibrous containing lignin copolymers stimulated cell proliferation in both BMSCs and Schwann cells, increased Schwann cell myelin basic protein expression, and stimulated neurite outgrowth in dorsal root ganglion neurons. Overall, these long-lasting, naturally antioxidant nanofibrous could be a promising candidate for nerve TE uses [145].

The primary goal of Rezaei et al.'s work was the creation of biologically and mechanically proper 3D printed scaffold for lung tissue engineering using chitosan/PCl bioink. Design-Expert software was used to investigate different compositions for 3D printing. The scaffolds were tested for MRC-5

 doi:10.20944/preprints202309.0709.v1



cell line growth, incrementation, and migration using chemical, biological, and mechanical methods. According to the findings, the average radius of the chitosan/PCL strands was 180 mm. Changes in PCL content had no effect on printability, whereas chitosan concentration did. The scaffolds demonstrated excellent swelling, degradation, and mechanical manner, but they can be altered by adjusting the PCL ingredient. In vitro, the scaffolds also demonstrated significant cell biocompatibility, nontoxicity, low apoptosis, high increment, and cell adhesion. To summarize, scaffold 3 (chitosan/PCL ratio: 4:1) demonstrated superior MRC-5 cell culture activity. As a result, this scaffold may be an excellent choice for lung tissue engineering [146].

There have been several attempts to combine biopolymers with inexpensive natural micro/nano particles such as lignin, alginate, and gums to create new substances with improved features. The technique of electrospinning (ELS) was used to create nanocomposites of lignin and PCL scaffold. Nanocomposite containing (0, 5, 10, and 15% wt%) lignin were produced by adding lignin powder to the PCL solution with stirring at RT. When compared to pure PCL, the scaffold with 10% lignin had suitable porosity, biodegradability, minimal fiber radius, ideal pore size, and improved tensile strength and elastic modulus. Degradation tests using samples immersed in phosphate-buffer saline revealed that the addition of lignin could accelerate degradation of PCL composites by up to 10% [147].

Zhang et al. presented novel, high-performance lignin-PCL-based polyurethane bioplastics. The PCL was added to the lignin as a biodegradable soft segment via a hexamethylene diisocyanate (HDI) bridge with long flexible aliphatic organic chains and high activity. Investigation was done into how the NCO/OH mole ratio, lignin content, and PCL molecular mass affected the characteristics of the resulting polyurethane plastics. It is crucial to note that the polyurethane film retained high tensile strength (19.35 MPa), elongation at break (188.36%), and tear strength (38.94 kN/m) when the lignin content reached 37.3%; additionally, it was remarkably stable at 340.8 °C and displayed exceptional solvent stability. An efficient method for enhancing lignin processability and creating sustainable bioplastic materials, like sealing compounds, biodegradable packaging films, and bio-adhesives, is the accomplished production of lignin-based polyurethane bioplastics [148].

By film casting, Kotcharat et al. created a PCL/bacterial cellulose (BC) composite with a specific ratio of 1%, 5%, 10%, 20%, 30%, and 50% v/v of BC. Alkaline purification was used to extract BC from nata de coco. The percentage of crystallinity decreased with increasing BC content. Porosity was discovered in the microstructure of the BC/PCL composite. It was noteworthy that the thermal decomposition manner remained stable up to 400 ◦C. When BC was added to DI water and phosphate buffered saline (PBS) solution, there was no significant change in swelling manner. Swelling and degradation features were studied for 6 hours and 4 weeks, respectively. As a result, PCL and BC-based composites can benefit significantly as exceptional candidates for wound dressing applications [149].

From a blend solution of PCL, cellulose acetate (CA) and dextran, an electrospun nanofibers mat for use in wound dressing was favorably created. The composite mat's antimicrobial activity, blood clotting capacity, cell attachment, and cell increment were all improved by the addition of a small quantity of the antibacterial medicine tetracycline hydrochloride. The composite's antimicrobial activity was tested using zone inhibition opposed to gram-positive and gram-negative bacteria, and the results show that it has a high antibacterial activity. As a result, the synthesized composite fiber has good properties for wound dressing and skin engineering uses [150].

According to Gorrasi et al., a new thermoplastic biodegradable compound (m-PCL-Pectin) was produced using a solvent-free method by altering natural pectin with m-PCL, a compound with pendants made of glycidyl methacrylate and maleic anhydride. Films were produced by processing the obtained material while it was still molten. The structural, thermal, mechanical, and barrier features to water vapor of pure pectin and modified PCL films were evaluated and compared. The suggested green method presents an excellent chance to produce fruit waste in order to get flexible and completly biodegradable polymers for food packaging uses, as an intriguing replacement for conventional thermoplastics that are not biodegradable. According to analysis of mechanical properties, pectin's high rigidity and stiffness, as shown by stress at break and elongation at break point, severely

Preprints (www.preprints.org) | NOT PEER-REVIEWED | Posted: 12 September 2023 doi:10.20944/preprints202309.0709.v1



restrict its use in the flexible packaging field. However, this limitation might be overcome thanks to the approach, as elongation at break is significantly increased [151].

The advancement of a PCL electrospun composite coated with pectin/polyaniline (PANi) that was elucidated and had a use for drug delivery, was described in the work of Hamzah et al. The SEM micrograph showed a powerful interaction between the bilayer structures and the interlinked porous of uniform fibers. The composition pectin(12%)/PANi(3%) was discovered as the maximized composition with a high tensile strength of 55.48±0.65 MPa and a modulus strength of 63.30±0.43 MPa at an electrical percolation of $2.4110^{-3}$ S/cm [152]. General usage of PCL, PCL-blends/composites can be summarized as shown in Figure 6.

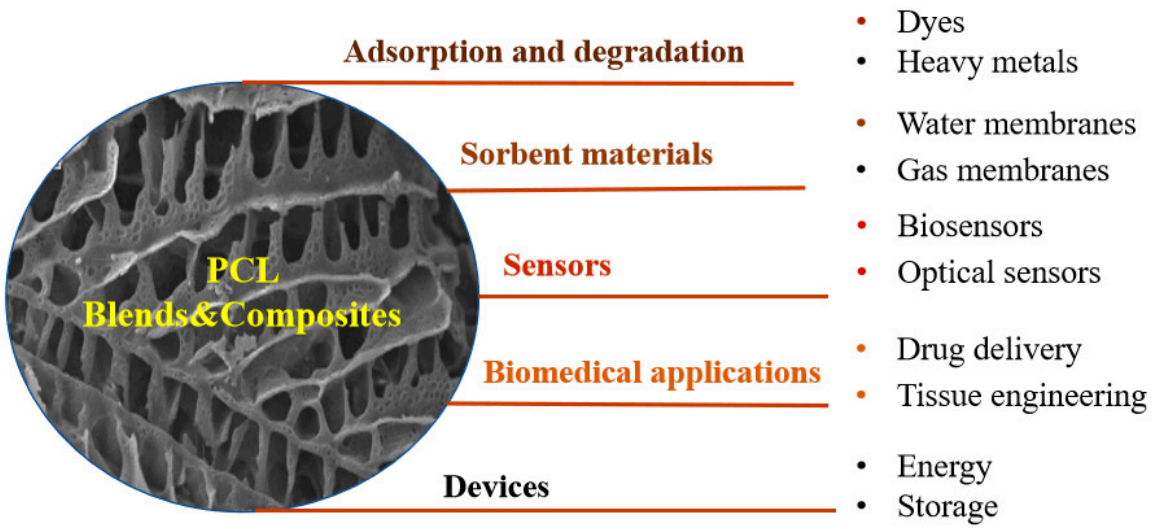


**Figure 6.** Usage of PCL based materials [25,73,139,153].

## 7. Conclusions

PCL is a biodegradable polymer commonly employed commercially in biomedical applications. However, it provides many advantages in the development of adsorbents for the removal of dyes and heavy metals. Over the last decade, there has been a significant increase in the use of PCL as an adsorbent in research, indicating its acceptance. This review surveyed recent advances in the fabrication of various forms of PCL blends and composites, and their applications in wastewater treatment. The removal of anionic/cationic dyes and heavy metal ions can be excellent options for producing low-cost PCL-based adsorbents with improved mechanical properties. Based on the data analyzed and discussed in this review, we can reach conclusion that PCL and its composites/blends provide an exciting and viable platform for the long-term generation of biodegradable adsorption materials. Furthermore, PCL can be a perfect choice for actively used adsorbents, particularly for eco-friendly antimicrobial adsorbents that require further investigation. The properties and use of PCL can be radically changed in a promising way by nanotechnology techniques. In comparison to other conventional techniques, it can be said that electrospinning processes are one of the most popular ways to prepare PCL for use in blend and composite production.

Despite significant efforts to create and enhance the unique structures and functions of PCL blends and composites used for wastewater treatment, many limitations remain. The parameters of the reaction medium and the surrounding environment have a large influence on the features of PCL, PCL-blends, and PCL-composites. As a result, the properties of the fabricated PCL-blends and PCL-composites like their environmental friendliness, degradability, processability, non-toxicity, mechanical and thermal features, as well as availability, long-term durability and cost-effectiveness are taken into account and further optimized in order to remove the other drawbacks. In addition, it should be investigated how to make more use of suspended PCL-blend and PCL-composites after dye and heavy metal removal processes to reduce overall costs. The synthesis of new and renewable PCL

blends and PCL composites with specific properties and mechanical properties as well as strong abilities in the purification of different pollutants from wastewater is becoming increasingly important.

**Author Contributions:** Gizem Özge Kayan: Data curation, Investigation, Drawing graphics, Formal analysis, Writing-original draft. Asgar Kayan: Conceptualization, Methodology, Resources, Supervision, Writing-Review Editing, Visualization.

**Funding:** No funding.

**Data Availability Statement:** All data generated or analyzed during this study are included in this published article.

**Acknowledgments:** The authors received no financial support for the research, authorship, and publication of this review article, but some facilities at Kocaeli University were used.

**Conflicts of interest:** The authors declare no conflict of interest.

## References

1. Zhang, H.; Pap, S.; Taggart, M.A.; Boyd, K.G.; James, N.A.; Gibb, S.W. A review of the potential utilisation of plastic waste as adsorbent for removal of hazardous priority contaminants from aqueous environments. *Environ. Pollut*. **2020**, *258*, 113698.
2. Moharir, R.V.; Kumar, S. Challenges associated with plastic waste disposal and allied microbial routes for its effective degradation: a comprehensive review. *J. Clean. Prod.* **2019**, *208*, 65-76.
3. Zhai, Z.; Du, X.; Zheng, H.; Long, Y. Biodegradable polymeric materials for flexible and degradable electronics. *Front. Electron.* **2022**, *3*, 985681.
4. Baranwal, J.; Barse, B.; Fais, A.; Delogu, G.L.; Kumar, A. Biopolymer: A sustainable material for food and medical applications. *Polymers* **2022**, *14*, 983.
5. Nanda, S.; Patra, B.R.; Patel, R.; Bakos, J.; Dalai, A.K. Innovations in applications and prospects of bioplastics and biopolymers: a review. *Environ. Chem. Lett*. **2022**, *20*, 379-395.
6. Kurakula, M.; Rao, G.K.; Yadav, K.S. Fabrication and characterization of polycaprolactone-based green materials for drug delivery. In Ahmed S (ed) Applications of Advanced Green Materials. Woodhead Publishing, Cambridge, **2021**, 395-423.
7. Siddiqui, N.; Kishori, B.; Rao, S.; Anjum, M.; Hemanth, V.; Das, S.; Jabbari, E. Electropsun polycaprolactone fibres in bone tissue engineering: a review. *Mol. Biotechnol.* **2021**, *63*, 363-388.
8. Hsissou, R.; Seghiri, R.; Benzekri, Z.; Hilali, M.; Rafik, M.; Elharfi, A. Polymer composite materials: A comprehensive review. *Compos. Struct*. **2021**, *262*, 113640.
9. Ghosal, K.; Manakhov, A.; Zajíčková, L.; Thomas, S. Structural and surface compatibility study of modified electrospun poly (ε-caprolactone)(PCL) composites for skin tissue engineering. *AAPS PharmSciTech*. **2017**, *18*, 72-81.
10. Olsen, P.; Herrera, N.; Berglund, L.A. Polymer grafting inside wood cellulose fibers by improved hydroxyl accessibility from fiber swelling. *Biomacromolecules* **2019**, *21*, 597-603.
11. de Oliveira Aguiar, V.; de Fatima Vieira Marques, M. Composites of polycaprolactone with cellulose fibers: morphological and mechanical evaluation. *Macromol. Symp.* **2016**, *367*, 101-112.
12. Ilyas, R.A.; Zuhri, M.Y.M.; Norrrahim, M.N.F.; Misenan, M.S.M.; Jenol, M.A.; Samsudin, S.A.; Omran, A.A.B. Natural fiber-reinforced polycaprolactone green and hybrid biocomposites for various advanced applications. *Polymers* **2022**, *14*, 182.
13. Deng, X.; Qasim, M.; Ali, A. Engineering and polymeric composition of drug-eluting suture: A review. *J. Biomed. Mater. Res A*. **2021**, *109*, 2065-2081.
14. El Fawal, G.; Hong, H.; Mo, X.; Wang, H. Fabrication of scaffold based on gelatin and polycaprolactone (PCL) for wound dressing application. *J. Drug. Deliv. Sci. Technol.* **2021**, *63*, 102501.
15. Moore, M.J.; Tan, R.P.; Yang, N.; Rnjak-Kovacina, J.; Wise, S.G. Bioengineering artificial blood vessels from natural materials. *Trends Biotechnol*. **2022**, *40*, 693-707.
16. Salehi, A.O.M.; Keshel, S.H.; Sefat, F.; Tayebi, L. Use of polycaprolactone in corneal tissue engineering: A review. *Mater. Today. Commun*. **2021**, *27*, 102402.
17. Banimohamad-Shotorbani, B.; Rahmani Del Bakhshayesh, A.; Mehdipour, A.; Jarolmasjed, S.; Shafaei, H. The efficiency of PCL/HAp electrospun nanofibers in bone regeneration: A review. *J. Med. Eng. Technol*. **2021**, *45*, 511-531.

18. Bangar, S.P.; Whiteside, W.S.; Ashogbon, A.O.; Kumar, M. Recent advances in thermoplastic starches for food packaging: A review. Food Packag. Shelf Life **2021**, *30*, 100743.
19. Sharma, V.; Borkute, G.; Gumfekar, S.P. Biomimetic nanofiltration membranes: Critical review of materials, structures, and applications to water purification. *Chem. Eng. J.* **2022**, *433*, 133823.
20. Arif, U.; Haider, S.; Haider, A.; Khan, N.; Alghyamah, A.A.; Jamila, N.; Kang, I.K. Biocompatible polymers and their potential biomedical applications: A review. *Curr. Pharm. Des*. **2019**, *25*, 3608-3619.
21. Müller, K.; Zollfrank, C.; Schmid, M. Natural polymers from biomass resources as feedstocks for thermoplastic materials. *Macromol. Mater. Eng*. **2019**, *304*, 1800760.
22. Labet, M.; Thielemans, W. Synthesis of polycaprolactone: a review. Chem. Soc. Rev. **2009**, *38*, 3484-3504.
23. Kayan, A. Recent studies on single site metal alkoxide complexes as catalysts for ring opening polymerization of cyclic compounds. Catal. Surv. Asia **2020**, *24*, 87-103.
24. Kaluzynski, K.; Pretula, J.; Lewinski, P.; Kaźmierski, S.; Penczek, S. Catalysis in polymerization of cyclic esters. Catalyst and initiator in one molecule. Polymerization of ε-caprolactone. *J. Catal*. **2020**, *392*, 97-107.
25. Thakur, M.; Majid, I.; Hussain, S.; Nanda, V. Poly (ε-caprolactone): A potential polymer for biodegradable food packaging applications. *Packag. Technol. Sci*. **2021**, *34*, 449-461.
26. Grobelny, Z.; Golba, S.; Jurek-Suliga, J. Mechanism of ε-caprolactone polymerization in the presence of alkali metal salts: investigation of initiation course and determination of polymers structure by MALDI-TOF mass spectrometry. *Polym. Bull*. **2019**, *76*, 3501-3515.
27. Cama, G.; Mogosanu, D.E. Houben, A.; Dubruel, P. Synthetic biodegradable medical polyesters: poly-ε-caprolactone. In: Zhang X (ed) Science and Principles of Biodegradable and Bioresorbable Medical Polymers, 1st edn. Woodhead Publishing, Cambridge, **2017**,79-105.
28. Penczek, S.; Pretula, J. Activated Monomer Mechanism (AMM) in Cationic Ring-Opening Polymerization. The Origin of the AMM and Further Development in Polymerization of Cyclic Esters. *ACS Macro. Lett*. *2021*, *10*, 1377-1397.
29. Jung, H.J.; Cho, Y.; Kim, D.; Mehrkhodavandi, P. Cationic aluminum, gallium, and indium complexes in catalysis. *Catal. Sci. Technol*. **2021**, *11*, 62-91.
30. Xu, Y.; Wang, L.; Chen, C.; Huang, P.; Dai, H.; Jiang, W.; Zhou, Y. Living Cationic Polymerization of ε-Caprolactone Catalyzed by a Metal-free Lewis Acid of Trityl Tetrafluoroborate. *Macromolecules* **2023**, *56*, 501-509.
31. Grobelny, Z.; Jurek-Suliga, J.; Golba, S. The influence of hydroxylic compounds on cationic polymerization of ε-caprolactone mediated by iron (III) chloride in tetrahydrofuran solution. *Polym. Bull.* **2023,** *80*, 6307-6326.
32. Stridsberg, K.M.; Ryner, M.; Albertsson, A.C. Controlled ring-opening polymerization: polymers with designed macromolecular architecture. *Adv. Polym. Sci*. **2002**, *157*, 41-65.
33. Punyodom, W.; Limwanich, W.; Meepowpan, P.; Thapsukhon, B. Ring-opening polymerization of ε-caprolactone initiated by tin (II) octoate/n-hexanol: DSC isoconversional kinetics analysis and polymer synthesis. *Des. Monomers Polym*. *2021*, *24*, 89-97.
34. McCollum, A.M.; Longo, A.M.; Stahl, A.E.; Butler, A.S.; Rheingold, A.L.; Cundari, T.R.; Fritsch, J.M. Synthesis, spectroscopy, and crystallography of mononuclear, five-coordinate aluminum complexes that act as cyclic ester polymerization initiators. *Polyhedron* **2021**, *204*, 115233.
35. Yildiz B.C.; Kayan, A. Preparation of single-site tin (IV) compounds and their use in the polymerization of ε-caprolactone. *Des. Monomer Polym*. **2017**, *20*, 89-96.
36. Gökalp, Y.; Kayan, A. Synthesis and characterization of Ti-/Zr-diphenylpropanedione complexes and their application in the ring opening polymerization of Ɛ-caprolactone. *J. Turk. Chem. Soc. A Chem*. **2018**, *5*, 1095-1104.
37. Yildiz, B.C.; Kayan, A. Ti (IV)-silyliminophenolate catalysts for ϵ-caprolactone and L-Lactide polymerization. *Sustain. Chem. Pharm*. **2021**, *21*, 100416.
38. Lyubov, D.M.; Tolpygin, A.O.; Trifonov, A.A. Rare-earth metal complexes as catalysts for ring-opening polymerization of cyclic esters. Coord. Chem. Rev. **2019**, *392*, 83-145.
39. Appavoo, D.; Omondi, B.; Guzei, I.A. van Wyk, J.L.; Zinyemba, O.; Darkwa, J. Bis (3, 5-dimethylpyrazole) copper (II) and zinc (II) complexes as efficient initiators for the ring opening polymerization of ε-caprolactone and d, l-lactide. *Polyhedron* **2014**, *69*, 55-60.
40. Paradiso, V.; Capaccio, V.; Lamparelli, D.H.; Capacchione, C. [OSSO]-bisphenolate metal complexes: A powerful and versatile tool in polymerization catalysis. *Coord. Chem. Rev*. **2021**, *429*, 213644.

41. Wang, X.; Thevenon, A.; Brosmer, J.L.; Yu, I.; Khan, S.I.; Mehrkhodavandi, P.; Diaconescu, P.L. Redox control of group 4 metal ring-opening polymerization activity toward L-lactide and ε-caprolactone. *J. Am. Chem. Soc*. **2014**, *136*, 11264-11267.
42. Shao, J.; Zhou, H.; Wang, Y.; Luo, Y.; Yao, Y. Lanthanum complexes stabilized by a pentadentate Schiff-base ligand: synthesis, characterization, and reactivity in statistical copolymerization of ε-caprolactone and L-lactide. *Dalton. Trans*. **2020**, *49*, 5842-5850.
43. Vidal, J.L.; Yavitt, B.M.; Wheeler, M.D.; Kolwich, J.L.; Donovan, L.N.; Sit, C.S.; Kerton, F.M. (2022) Biochar as a sustainable and renewable additive for the production of Poly (ε-caprolactone) composites. *Sustain. Chem. Pharm*. **2022**, *25*, 100586.
44. Heimowska, A.; Morawska, M.; Bocho-Janiszewska, A. Biodegradation of poly (ε-caprolactone) in natural water environments. *Pol. J. Chem. Technol*. **2017**, *19*, 120-126.
45. Khan, I.; Dutta, J.R.; Ganesan, R. Lactobacillus sps. lipase mediated poly (ε-caprolactone) degradation. *Int. J. Biol. Macromol*. **2017**, *95*, 126-131.
46. Aris, M.H.; Annuar, M.S.M.; Ling, T.C. Lipase-mediated degradation of poly-ε-caprolactone in toluene: Behavior and its action mechanism. *Polym. Degrad. Stab*. **2016**, *133*, 182-191.
47. Ma, Q.; Shi, K.; Su, T.; Wang, Z. Biodegradation of polycaprolactone (PCL) with different molecular weights by Candida antarctica lipase. *J. Polym. Environ*. **2020**, *28*, 2947-2955.
48. Woodard, L.N. Grunlan, M.A. Hydrolytic degradation and erosion of polyester biomaterials. *ACS Macro. Lett*. **2018**, *7*, 976-982.
49. Singh, N.K.; Purkayastha, B.D.; Roy, J.K.; Banik, R.M.; Yashpal, M.; Singh, G.; Maiti, P. Nanoparticle-induced controlled biodegradation and its mechanism in poly (ε-caprolactone). *ACS Appl. Mater. Interfaces*. **2010**, *2*, 69-81.
50. Tyagi, P,; Agate, S.; Velev, O.D.; Lucia. L.; Pal. L. A critical review of the performance and soil biodegradability profiles of biobased natural and chemically synthesized polymers in industrial applications. *Environ. Sci. Technol*. **2022**, *56*, 2071-2095.
51. Liu, Q.; Yuan, S.; Guo, Y.; Narayanan, A.; Peng, C.; Wang, S.; Joy, A. Modulating the crystallinity, mechanical properties, and degradability of poly (ε-caprolactone) derived polyesters by statistical and alternating copolymerization. *Polym. Chem.* **2019**, *10*, 2579-2588.
52. Magazzini, L.; Grilli, S.; Fenni, S.E.; Donetti, A.; Cavallo, D.; Monticelli, O. The Blending of Poly (glycolic acid) with Polycaprolactone and Poly (l-lactide): Promising Combinations. *Polymers* **2021**, *13*, 2780.
53. Mohamed, R.M.; Yusoh, K. A review on the recent research of polycaprolactone (PCL). Trans Tech Publications Ltd. *In Adv Mater Res*. **2016**, *1134*, 249-255.
54. Sin, L.T.; Rahmat, A.R.; Rahman, W.A. In: Ebnesajjad S(ed) Handbook of Biopolymers and Biodegradable Plastics, 1st edn. Elsevier, Amsterdam, **2013,** 11-54.
55. Guarino, V.; Gentile, G.; Sorrentino, L.; Ambrosio, L. Polycaprolactone: synthesis, properties, and applications. *Encyclopedia Polym. Sci. Technol*. **2017**, 1-36.
56. Espinoza, S.M.; Patil, H.I.; San Martin Martinez, E.; Casañas Pimentel, R.; Ige, P.P. Poly-ε-caprolactone (PCL), a promising polymer for pharmaceutical and biomedical applications: Focus on nanomedicine in cancer. *Int. J. Polymeric Mater. Polym. Biomater*. **2020**, *69*, 85-126.
57. Homaeigohar, S.; Boccaccini, A.R. Nature-Derived and Synthetic Additives to poly (ε-Caprolactone) Nanofibrous Systems for Biomedicine; an Updated Overview. *Front. Chem*. **2022**, *9*, 809676.
58. Bartnikowski, M.; Dargaville, T.R. Ivanovski, S.; Hutmacher, D.W. Degradation mechanisms of polycaprolactone in the context of chemistry, geometry and environment. *Prog. Polym. Sci.* **2019**, *96*, 1-20.
59. Taniguchi, H.; Kurokawa, N.; Inukai, S.; Hotta, A. Structures and mechanical properties of electrospun cellulose nanofibers/poly (ε-caprolactone) composites. *J. Appl. Polym. Sci.* **2020**, *137*, 49307.
60. Clamor, C.; Cattoz, B.N.; Wright, P.M.; O'Reilly, R.K.; Dove, A.P. Controlling the crystallinity and solubility of functional PCL with efficient post-polymerisation modification. *Polym. Chem*. **2021**, *12*, 1983-1990.
61. Goel, V.; Luthra, P.; Kapur, G.S.; Ramakumar, S.S.V. Biodegradable/bio-plastics: myths and realities. *J. Polym. Environ*. **2021**, *29*, 3079-3104.
62. Nandakumar, A.; Chuah, J.A.; Sudesh, K. Bioplastics: a boon or bane? Renew. Sustain. Energy Rev. **2021**, *147*, 111237.
63. Moshood, T.D.; Nawanir, G.; Mahmud, F.; Mohamad, F.; Ahmad, M.H.; AbdulGhani, A. Sustainability of biodegradable plastics: New problem or solution to solve the global plastic pollution. *Curr. Res. Green Sustain. Chem*. **2022**, *5*, 100273.

64. Adeli-Sardou, M.; Yaghoobi, M.M.; Torkzadeh-Mahani, M.; Dodel, M. Controlled release of lawsone from polycaprolactone/gelatin electrospun nano fibers for skin tissue regeneration. *Int. J. Biol. Macromol*. **2019**, *124*, 478-491.
65. Leonés, A.; Mujica-Garcia, A.; Arrieta, M.P.; Salaris, V.; Lopez, D.; Kenny, J.M.; Peponi, L. Organic and inorganic PCL-based electrospun fibers. *Polymers* **2020**, *12*, 1325.
66. Faruk, O.; Bledzki, A.K.; Fink, H.P.; Sain, M. Biocomposites reinforced with natural fibers: 2000–2010. *Prog. Polym. Sci*. **2012**, *37*, 1552-1596.
67. Ludueña, L.; Vázquez, A.; Alvarez, V. Effect of lignocellulosic filler type and content on the behavior of polycaprolactone based eco-composites for packaging applications. *Carbohydr. Polym*. **2012**, *87*, 411-421.
68. Boujemaoui, A.; Cobo Sanchez, C.; Engstro¨m, J.; Bruce, C.; Fogelstro¨m, L.; Carlmark, A.; Malmstro¨m, E. Polycaprolactone nanocomposites reinforced with cellulose nanocrystals surface-modified via covalent grafting or physisorption: a comparative study. *ACS Appl. Mater. Interfaces* **2017**, *9*, 35305-35318.
69. Morouço, P.; Biscaia, S.; Viana, T.; Franco, M.; Malça, C.; Mateus, A.; Alves, N.M. Fabrication of Poly (-caprolactone) Scaffolds Reinforced with Cellulose Nanofibers, with and without the Addition of Hydroxyapatite Nanoparticles. *BioMed. Res. Int.* **2016**, *2016*, 1596157.
70. Yu, Y.; Gao, X.; Jiang, Z.; Zhang, W.; Ma, J.; Liu, X.; Zhang, L. Homogeneous grafting of cellulose with polycaprolactone using quaternary ammonium salt systems and its application for ultraviolet-shielding composite films. *RSC Adv.* **2018**, *8*, 10865-10872.
71. Mi, H.Y.; Jing, X.; Peng, J.; Salick, M.R.; Peng, X.F. Turng, L.S. Poly (ε-caprolactone)(PCL)/cellulose nanocrystal (CNC) nanocomposites and foams. *Cellulose* **2014**, *21*, 2727-2741.
72. Hashiwaki, H.; Teramoto, Y.; Nishio, Y. Fabrication of thermoplastic ductile films of chitin butyrate/poly (ε-caprolactone) blends and their cytocompatibility. *Carbohydr. Polym*. **2014**, 114, 330-338.
73. Malikmammadov, E.; Tanir, T.E.; Kiziltay, A.; Hasirci, V.; Hasirci, N. PCL and PCL-based materials in biomedical applications. *J. Biomater. Sci. Polym. Ed*. **2018**, *29*, 863-893.
74. San, I.S.; Rezaei, M.; Khoshfetrat, A.B.; Razzaghi, D. Preparation and characterization of polycaprolactone/chitosan-g-polycaprolactone/hydroxyapatite electrospun nanocomposite scaffolds for bone tissue engineering. *Int. J. Biol. Macromol*. **2021**, *182*, 1638-1649.
75. Manoel, A.F.; Claro, P.I.; Galvani, F.; Mattoso, L.H.; Marconcini, J.M.; Mantovani, G.L. Poly (ε-caprolactone) blended with thermoplastic waxy starch matrix reinforced with cellulose nanocrystals from Macauba (Acrocomia spp.) Rachis. *Ind. Crops. Prod*. **2022**, *177*, 114446.
76. Peterson, C.H.; Werber, J.R.; Lee, H.K.; Hillmyer, M.A. Tailored Mesoporous Microspheres by Polymerization-Induced Microphase Separation in Suspension. *ACS Appl. Polym. Mater.* 2022, *4*, 4219-4233.
77. Li, W.; Zong, Y.; Liu, Q.; Sun, Y.; Li, Z.; Wang, H.; Li, Z. A highly stretchable and biodegradable superamphiphobic fluorinated polycaprolactone nanofibrous membrane for antifouling. *Prog. Org. Coat*. **2020**, *147*, 105776.
78. Rusli, M.S.I.C.; Hassan, M.I.; Sultana, N.; Ismail, A.F. Characterization of PCL/zeolite electrospun membrane for the removal of silver in drinking water. *J. Teknol*. **2017**, *79*, 89-95.
79. Huang, Y.; Dan, N.; Dan, W.; Zhao, W. Reinforcement of polycaprolactone/chitosan with nanoclay and controlled release of curcumin for wound dressing. *ACS Omega.* **2019**, *4*, 22292-22301.
80. Karimian, R.; Mehrabani, M.G.; Mehramuz, B.; Ganbarov, K.; Ejlali, L.; Tanomand, A.; Kafil, H.S. Poly (ε-Caprolactone)/cellulose nanofiber blend nanocomposites containing $ZrO_2$ nanoparticles: A new biocompatible wound dressing bandage with antimicrobial activity. *Adv. Pharm. Bull*. **2020**, *10*, 577.
81. Ramírez-Cedillo, E.; Ortega-Lara, W.; Rocha-Pizaña, M.R.; Gutierrez-Uribe, J.A.; Elías-Zúñiga, A.; Rodríguez, C.A. Electrospun polycaprolactone fibrous membranes containing Ag, $TiO_2$ and $Na_2Ti_6O_{13}$ particles for potential use in bone regeneration. *Membranes* **2019**, *9*, 12.
82. del Ángel-Sánchez, K.; Borbolla-Torres, C.I.; Palacios-Pineda, L.M.; Ulloa-Castillo, N.A.; Elías-Zúñiga, A. Development, fabrication, and characterization of composite polycaprolactone membranes reinforced with $TiO_2$ nanoparticles. *Polymers* **2019**, *11*, 1955.
83. Scaffaro, R.; Gammino, M.; Maio, A. Wet electrospinning-aided self-assembly of multifunctional GO-CNT@ PCL core-shell nanocomposites with spider leg bioinspired hierarchical architectures. *Compos. Sci. Technol*. **2022**, *221*, 109363.
84. Thamer, B.M.; Aldalbahi, A.; Moydeen, A.M.; Rahaman, M.; El-Newehy, M.H. Modified electrospun polymeric nanofibers and their nanocomposites as nanoadsorbents for toxic dye removal from contaminated waters: A review. *Polymers* **2021**, *13*, 20.

85. Guo, R.; Wang, R.; Yin, J.; Jiao, T.; Huang, H.; Zhao, X.; Peng, Q. Fabrication and highly efficient dye removal characterization of beta-cyclodextrin-based composite polymer fibers by electrospinning. *Nanomaterials* **2019**, *9*, 127.
86. Zdarta, J.; Staszak, M.; Jankowska, K.; Kaźmierczak, K.; Degórska, O.; Nguyen, L.N.; Jesionowski, T. The response surface methodology for optimization of tyrosinase immobilization onto electrospun polycaprolactone–chitosan fibers for use in bisphenol A removal. *Int. J. Biol. Macromol*. **2020**, *165*, 2049-2059.
87. Chen, J.; Xiang, C.; He, N.; Zhang, J.; Li, L.; Dong, S. Chitosan/poly (ε-caprolactone)-block-poly (ethylene glycol) copolymer electrospun membrane for the adsorption of dyes. *New. J. Chem*. **2020**, *44*, 20458-20469.
88. Draoua, Z.; Harrane, A.; Adjdir, M. Preparation, characterization and application of the nanocomposite PCL-PEG-PCL/Bentonite for the removal of methylene blue (MB) dye. *Res. Chem. Intermed*. *2021*, *47*, 4635-4655.
89. Karagoz, S.; Kiremitler, N.B.; Sakir, M.; Salem, S.; Onses, M.S.; Sahmetlioglu, E.; Yilmaz, E. Synthesis of Ag and $TiO_2$ modified polycaprolactone electrospun nanofibers (PCL/$TiO_t$-Ag NFs) as a multifunctional material for SERS, photocatalysis and antibacterial applications. *Ecotoxicol. Environ. Saf*. **2020**, *188*, 109856.
90. Nivedita, S.; Joseph, S. Optimization of process parameters using response surface methodology for PCL based biodegradable composite membrane for water purification. *Arab. J. Sci. Eng*. **2020**, *45*, 7347-7360.
91. Sarioglu, O.F.; San Keskin, N.O.; Celebioglu, A.; Tekinay, T.; Uyar, T. Bacteria immobilized electrospun polycaprolactone and polylactic acid fibrous webs for remediation of textile dyes in water. *Chemosphere* **2017**, *184*, 393-399.
92. Wang, C.; Yin, J.; Wang, R.; Jiao, T.; Huang, H.; Zhou, J.; Peng, Q. Facile preparation of self-assembled polydopamine-modified electrospun fibers for highly effective removal of organic dyes. *Nanomaterials* **2019**, *9*, 116.
93. Scaffaro, R.; Gammino, M.; Maio, A. Wet electrospinning-aided self-assembly of multifunctional GO-CNT@PCL core-shell nanocomposites with spider leg bioinspired hierarchical architectures. *Compos. Sci. Technol*. **2022**, *221*, 109363.
94. Yousfi, R.E.; Achalhi, N.; Benahmed, A.; El Idrissi, A. Synthesis, characterization of multi-arm copolymers and linear blocks based on PEG and PCL: Effect of topology on dye adsorption. *Mater. Today: Proc.* **2023**, *72*, 3650-3661.
95. Xue, W.; Hu, Y.; Wang, F.; Yang, X.; Wang, L. $Fe_3O_4$/poly (caprolactone)(PCL) electrospun membranes as methylene blue catalyst with high recyclability. *Colloids Surf. A: Physicochem. Eng. Asp*. **2019**, *564*, 115-121.
96. Alrafai, H.A.; Al-Ahmed, Z.A.; Ahmed, M.K.; Afifi, M.; Shoueir, K.R.; Abu-Rayyan, A. The degradation of methylene blue dye using copper-doped hydroxyapatite encapsulated into polycaprolactone nanofibrous membranes. *New J. Chem*. **2021**, *45*, 16143-16154.
97. Elias, E.; Sarathchandran, C.; Joseph, S.; Zachariah, A.K.; Thomas, J.; Devadasan, D.; Thomas, S. Photoassisted degradation of rhodamine B using poly (ε-caprolactone) based nanocomposites: Mechanistic and kinetic features. *J. Appl. Polym. Sci*. **2021**, *138*, 50612.
98. Marković, D.; Milovanović, S.; Radoičić, M.B.; Radovanović, Ž.; Žižović, I.T.; Šaponjić, Z.; Radetić, M.M. Removal of textile dyes from water by $TiO_2$ nanoparticles immobilized on poly (ε-caprolactone) beads and foams. *J. Serb. Chem. Soc.* **2018**, *83*, 1379-1389.
99. Geravand, M.H.A.; Saljoughi, E.; Mousavi, S.M.; Kiani, S. Biodegradable polycaprolactone/MXene nanocomposite nanofiltration membranes for the treatment of dye solutions. *J. Taiwan Inst. Chem. Eng*. **2021**, *128*, 124-139.
100. Tu, H.; Li, D.; Yi, Y.; Liu, R.; Wu, Y.; Dong, X.; Deng, H. Incorporation of rectorite into porous polycaprolactone/$TiO_2$ nanofibrous mats for enhancing photocatalysis properties towards organic dye pollution. *Compos. Commun*. **2019**, *15*, 58-63.
101. Xie, J.; Hung, Y.C. UV-A activated $TiO_2$ embedded biodegradable polymer film for antimicrobial food packaging application. *Lwt* **2018**, *96*, 307-314.
102. Saeed, K.; Khan, N.; Shah, T.; Sadiq, M. Morphology, Properties and Application of Iron Oxide/Polycaprolactone Nanocomposites. *J. Chem. Soc. Pak.* **2021**, *43*, 34-40.
103. Yan, B.; Wang, X.; Zhang, X.; Liu, S.; Lu, H.; Ran, R. One-step preparation of hydroxyapatite-loaded magnetic Polycaprolactone hollow microspheres for malachite green adsorption by Pickering emulsion template method. *Colloids Surf. A: Physicochem. Eng. Asp*. **2022**, *639*, 128347.

104. Chen, J.; Liu, L. Huang, J.; Sheng, C.; Li, L. Porous multicomponent chitosan/poly (ε-caprolactone)-block poly (ethylene glycol)/$SiO_2$ aerogel@ polydopamine membrane for Congo red adsorption. *Mater. Today Chem*. **2022**, *23*, 100661.
105. Radwan, H.A.; Ismail, R.A. Abdelaal, S.A.; Al Jahdaly, B.A.; Almahri, A.; Ahmed, M.K.; Shoueir, K. Electrospun polycaprolactone nanofibrous webs containing Cu–Magnetite/Graphene oxide for cell viability, antibacterial performance, and dye decolorization from aqueous solutions. *Arab. J. Sci. Eng*. **2022**, *47*, 303-318.
106. Xue, W.; Hu, Y.; Wang, F.; Yang, X.; Wang, L. $Fe_3O_4$/poly (caprolactone)(PCL) electrospun membranes as methylene blue catalyst with high recyclability. Colloids Surf. A: Physicochem. Eng. Asp. **2019**, *564*, 115-121.
107. Pekdemir, M.E.; Tanyol, M.; Torğut, G. Preparation of ε-Caprolactone/$Fe_3O_4$ Magnetic Nanocomposite and Its Application to the Remazol Brilliant Violet 5R Dye Adsorption from Wastewaters by Using RSM. *J. Polym. Environ*. **2022**, *30*, 4225-4237.
108. He, N.; Li, L.; Chen, J.; Zhang, J.; Liang, C. Extraordinary superhydrophobic polycaprolactone-based composite membrane with an alternated micro–nano hierarchical structure as an eco-friendly oil/water separator. *ACS Appl. Mater. Interfaces* **2021**, *13*, 24117-24129.
109. Uzunok, S.; Sonmez, H.B. Reusable polycaprolactone based sorbents with different cross-linking densities for the removal of organic pollutants. *J. Environ. Chem. Eng*. **2023**, *11*, 109287.
110. Eom, J.; Kwak, Y.; Nam, C. Electrospinning fabrication of magnetic nanoparticles-embedded polycaprolactone (PCL) sorbent with enhanced sorption capacity and recovery speed for spilled oil removal. *Chemosphere* **2022**, *303*, 135063.
111. Seema, K.M.; Mamba, B.B.; Njuguna, J.; Bakhtizin, R.Z.; Mishra, A.K. Removal of lead (II) from aqueous waste using (CD-PCL-$TiO_2$) bio-nanocomposites. *Int. J. Biol. Macromol*. **2018**, *109*, 136-142.
112. Liakos, I.L.; Mondini, A.; Del Dottore, E.; Filippeschi, C.; Pignatelli, F.; Mazzolai, B. 3D printed composites from heat extruded polycaprolactone/sodium alginate filaments and their heavy metal adsorption properties. *Mater. Chem. Front*. **2020**, *4*, 2472-2483.
113. Aquino, R.R.; Tolentino, M.S.; Elacion, R.M.P.D.; Ladrillono, R.; Laurenciana, T.R.C.; Basilia, B.A. Adsorptive removal of lead (Pb2+) ion from water using cellulose acetate/polycaprolactone reinforced nanostructured membrane. *In IOP Conf. Ser: Earth Environ. Sci*. **2018**, *191*, 012139.
114. Ma, L.; Shi, X.; Zhang, X.; Dong, S.; Li, L. Electrospun cellulose acetate–polycaprolactone/chitosan core–shell nanofibers for the removal of Cr (VI). *Phys. Status Solidi (a)* **2019**, *216*, 1900379.
115. Benhacine, F.; Abdellaoui, N.; Arous, O.; Hadj-Hamou, A.S. Behaviours of poly (ε-caprolactone)/silver-montmorillonite nanocomposite in membrane ultrafiltration for wastewater treatment. *Environ. Technol*. **2020**, *41*, 2049-2060.
116. Irandoost, M.; Pezeshki-Modaress, M.; Javanbakht, V. Removal of lead from aqueous solution with nanofibrous nanocomposite of polycaprolactone adsorbent modified by nanoclay and nanozeolite. *J. Water Process Eng*. **2019,** *32*, 100981.
117. Palacios Hinestroza, H.; Urena-Saborio, H.; Zurita, F.; Guerrero de Leon, A.A.; Sundaram, G.; Sulbarán-Rangel, B. Nanocellulose and polycaprolactone nanospun composite membranes and their potential for the removal of pollutants from water. *Molecules* **2020**, *25*, 683.
118. Lan, X.; Wang, H.; Liu, Y.; Chen, X.; Xiong, J.; Mai, R.; Tang, Y. Biodegradable trilayered micro/nano-fibrous membranes with efficient filtration, directional moisture transport and antibacterial properties. *Chem. Eng. J*. **2022**, *447*, 137518.
119. Song, W.; Qian, L.; Gao, B.; Zhu, Y.; Zhu, M.; Zhao, Y.; Miao, Z. Ionic liquid-based amphiphilic conetwork with mechanical toughness: a promising candidate for dye removal. *J. Mater. Sci*. **2019**, *54*, 6212-6226.
120. Kayan, G.O.; Kayan, A. Inorganic–Organic Hybrid Materials of Zirconium and Aluminum and Their Usage in the Removal of Methylene Blue. *J. Inorg. Organomet. Polym. Mater*. **2021**, *31*, 3613-3623.
121. Kayan, G.O.; Kayan, A. Polyhedral Oligomeric Silsesquioxane and Polyorganosilicon Hybrid Materials and Their Usage in the Removal of Methylene Blue Dye. *J. Inorg. Organomet. Polym. Mater*. **2022**, *32*, 2781-2792.
122. Mohammad, N.; Atassi, Y. Adsorption of methylene blue onto electrospun nanofibrous membranes of polylactic acid and polyacrylonitrile coated with chloride doped polyaniline. *Sci. Rep*. **2020**, *10*, 13412.
123. Bahalkeh, F.; Mehrabian, R.Z.; Ebadi, M. Removal of Brilliant Red dye (Brilliant Red E-4BA) from wastewater using novel Chitosan/SBA-15 nanofiber. *Int. J. Biol. Macromol*. **2020**, *164*, 818-825.

124. Qi, F.F.; Ma, T.Y.; Liu, Y.; Fan, Y.M.; Li, J.Q.; Yu, Y.; Chu, L.L. 3D superhydrophilic polypyrrole nanofiber mat for highly efficient adsorption of anionic azo dyes. *Microchem. J*. **2020**, *159*, 105389.
125. Lin, Y.; Tian, Y.; Sun, H.; Hagio, T. Progress in modifications of 3D graphene-based adsorbents for environmental applications. *Chemosphere* **2021**, *270*, 129420.
126. Kayan, G.O.; Kayan, A. Composite of natural polymers and their adsorbent properties on the dyes and heavy metal ions. *J. Polym. Environ*. **2021**, *29*, 3477-3496.
127. Baig, M.T.; Kayan, A. Eco-friendly novel adsorbents composed of hybrid compounds for efficient adsorption of methylene blue and Congo red dyes: Kinetic and thermodynamic studies. Sep. Sci. Technol. **2023**, *58*, 862-883.
128. Hussain, Z.; Ullah, S.; Yan, J.; Wang, Z.; Ullah, I.; Ahmad, Z.; Pei, R. Electrospun tannin-rich nanofibrous solid-state membrane for wastewater environmental monitoring and remediation. *Chemosphere* **2022**, *307*, 135810.
129. Lee, J.S.; Lee, H.B.; Oh, Y.; Choi, A.J.; Seo, T.H.; Kim, Y.K.; Lee, M.W. Used coffee/PCL composite filter for Cu (II) removal from wastewater. *J. Water Process Eng*. **2022**, *50*, 103253.
130. Ramírez-Rodríguez, L.C.; Quintanilla-Carvajal, M.X.; Mendoza-Castillo, D.I.; Bonilla-Petriciolet, A. Jiménez-Junca, C. Preparation and Characterization of an Electrospun Whey Protein/Polycaprolactone Nanofiber Membrane for Chromium Removal from Water. *Nanomaterials* **2022**, *12*, 2744.
131. Dela Peña, E.M.B.; Araño, K.; Dela Cruz, M.L.; de Yro, P.A.; Diaz, L.J.L. The design of a bench-scale adsorbent column based on nanoclay-loaded electrospun fiber membrane for the removal of arsenic in wastewater. *Water Environ. J.* **2021**, *35*, 937-942.
132. Mabborang, C.M.P.; Padrigo, J.N.B.; Quiachon, G.M.; de Yro, P.A.N. Synthesis and Characterization of Electrospun Carbon Quantum Dots–Polyacrylonitrile/Polycaprolactone Composite Nanofiber Membranes for Copper (II) Adsorption. *Key Eng. Mater*. **2021**, *878*, 3-8.
133. Tonsomboon, K.; Noppakuadrittidej, P.; Sutikulsombat, S.; Petdum, A.; Panchan, W.; Wanichacheva, N.; Karoonuthaisiri, N. Turn-On fluorescence resonance energy transfer (FRET)-based electrospun fibrous membranes: Rapid and ultrasensitive test strips for on-site detection of Mercury (II) ion. *Sens. Actuators B: Chem.* **2021**, *344*, 130212.
134. Bernhardt, K.T.; Collins, H.G.; Balija, A.M. Biorenewable triblock copolymers consisting of l-lactide and ε-caprolactone for removing organic pollutants from water: a lifecycle neutral solution. *BMC chem*. **2019**, *13*, 122.
135. Domingues, J.T.; Orlando, R.M.; Sinisterra, R.D.; Pinzon-Garcia, A.D.; Rodrigues, G.D. Polymer-bixin nanofibers: A promising environmentally friendly material for the removal of dyes from water. *Sep. Purif. Technol*. **2020**, *248*, 117118.
136. Kolak, S.; Birhanlı, E.; Boran, F.; Bakar, B.; Ulu, A.; Yeşilada, Ö.;, Ateş, B. Tailor-made novel electrospun polycaprolactone/polyethyleneimine fiber membranes for laccase immobilization: An all-in-one material to biodegrade textile dyes and phenolic compounds. *Chemosphere* **2023**, *313*, 137478.
137. Roque-Ruiz, J.H.; Cabrera-Ontiveros, E.A.; Torres-Pérez, J.; Reyes-López, S.Y. Preparation of PCL/clay and PVA/clay electrospun fibers for cadmium (Cd+2), chromium (Cr+3), copper (Cu+2) and lead (Pb+2) removal from water. *Water Air Soil Pollut*. **2016**, *227*, 286.
138. Saberi, R.; Sadjadi, S.; Ammari Allahyari, S.; Charkhi, A. Poly (ε-caprolactone) electrospun nanofibers decorated with copper hexacyanoferrate as an ion exchanger for effective cesium ion removal. *Sep. Sci. Technol*. **2022**, *57*, 897-909.
139. Zhang, D.; Wang, D.; Li, J.; Xu, X.; Zhang, H.; Duan, R.; Dong, B. One-step synthesis of PCL/Mg Janus micromotor for precious metal ion sensing, removal and recycling. *J. Mater. Sci*. **2019,** *54*, 7322-7332.
140. Somera, L.R.; Cuazon, R.; Cruz, J.K.; Diaz, L.J. Kinetics and isotherms studies of the adsorption of Hg (II) onto iron modified montmorillonite/polycaprolactone nanofiber membrane. *IOP Conf. Ser.: Mater. Sci. Eng*. **2019**, *540*, 012005.
141. Ataie, M.; Nourmohammadi, J.; Seyedjafari, E. Carboxymethyl carrageenan immobilized on 3D-printed polycaprolactone scaffold for the adsorption of calcium phosphate/strontium phosphate adapted to bone regeneration. *Int. J. Biol. Macromol*. **2022**, *206*, 861-874.
142. Körpınar, B.; Yayayürük, A.E.; Yayayürük, O.; Akat, H. Thiol–ended polycaprolactone: synthesis, preparation and use in Pb (II) and Cd (II) removal from water samples. *Mater. Today Commun*. **2021**, *29*, 102908.
143. Echeverria Molina, M.I.; Malollari, K.G.; Komvopoulos, K. Design challenges in polymeric scaffolds for tissue engineering. *Front. Bioeng. Biotechnol*. **2021**, *9*, 617141.

144. Das, P.; Remigy, J.C.; Lahitte, J.F. van der Meer, A.D.; Garmy-Susini, B.; Coetsier, C.; Bacchin, P. Development of double porous poly (ε-caprolactone)/chitosan polymer as tissue engineering scaffold. *Mater. Sci. Eng. C* **2020**, *107*, 110257.
145. Wang, J.; Tian, L.; Luo, B.; Ramakrishna, S.; Kai, D.; Loh, X.J.; Mo, X. Engineering PCL/lignin nanofibers as an antioxidant scaffold for the growth of neuron and Schwann cell. *Colloids Surf. B: Biointerfaces* **2018**, *169*, 356-365.
146. Rezaei, F.S.; Khorshidian, A.; Beram, F.M.; Derakhshani, A.; Esmaeili, J.; Barati, A. 3D printed chitosan/polycaprolactone scaffold for lung tissue engineering: Hope to be useful for COVID-19 studies. *RSC Adv*. **2021**, *11*, 19508-19520.
147. Salami, M.A.; Kaveian, F.; Rafienia, M.; Saber-Samandari, S.; Khandan, A.; Naeimi, M. Electrospun polycaprolactone/lignin-based nanocomposite as a novel tissue scaffold for biomedical applications. *J. Medical Signals Sens*. **2017**, *7*, 228.
148. Zhang, Y.; Liao, J.; Fang, X.; Bai, F.; Qiao, K.; Wang, L. Renewable high-performance polyurethane bioplastics derived from lignin–poly (ε-caprolactone). *ACS Sustain. Chem. Eng*. **2017**, *5*, 4276-4284.
149. Kotcharat, P.; Chuysinuan, P.; Thanyacharoen, T.; Techasakul, S.; Ummartyotin, S. Development of bacterial cellulose and polycaprolactone (PCL) based composite for medical material. *Sustain. Chem. Pharm*. **2021**, *20*, 100404.
150. Liao, N.; Unnithan, A.R.; Joshi, M.K.; Tiwari, A.P.; Hong, S.T.; Park, C.H.; Kim, C.S. Electrospun bioactive poly (ε-caprolactone)–cellulose acetate–dextran antibacterial composite mats for wound dressing applications. *Colloids Surf. A: Physicochem. Eng. Asp.* **2015**, *469*, 194-201.
151. Gorrasi, G.; Bugatti, V.; Viscusi, G.; Vittoria, V. Physical and barrier properties of chemically modified pectin with polycaprolactone through an environmentally friendly process. *Colloid. Polym. Sci*. **2021**, *299*, 429-437.
152. Hamzah, M.S.A.; Austad, A.; Abd Razak, S.I.; Nayan, N.H.M. Tensile and wettability properties of electrospun polycaprolactone coated with pectin/polyaniline composite for drug delivery application. *Int. J. Struct. Integr*. **2019**, *10*, 704-713.
153. Homocianu, M.; Pascariu, P. Electrospun polymer-inorganic nanostructured materials and their applications. *Polym. Rev*. **2020**, *60*, 493-541.